OXFORD

Dissecting structural connectivity of the left and right inferior frontal cortex in children who stutter

Nicole E. Neef (ID)[1,*], Mike Angstadt (ID)[2], Simone P.C. Koenraads (ID)[3,4], Soo-Eun Chang (ID)[2,5,6,*]

[1]Institute for Diagnostic and Interventional Neuroradiology, University Medical Center Göttingen, Robert-Koch-Straße 40, 37075 Göttingen, Germany,
[2]Department of Psychiatry, University of Michigan, 4250 Plymouth Road, Ann Arbor, MI 48105, USA,
[3]Department of Otorhinolaryngology and Head and Neck Surgery, Erasmus University Medical Center, Dr. Molewaterplein 40, 3015 GD Rotterdam, the Netherlands,
[4]The Generation R Study Group, Erasmus University Medical Center, Rotterdam, Wytemaweg 80, 3015 CN Rotterdam, the Netherlands,
[5]Department of Communicative Sciences and Disorders, Michigan State University, 1026 Red Cedar Road, East Lansing, MI 48824, USA,
[6]Cognitive Imaging Research Center, Department of Radiology, Michigan State University, 846 Service Road, East Lansing, MI 48824, USA

*Corresponding authors: Institute for Diagnostic and Interventional Neuroradiology, University Medical Center Göttingen, Robert-Koch-Straße 40, 37075 Göttingen, Germany. Email: nicole.neef@med.uni-goettinge.de (Nicole E. Neef); Department of Psychiatry, University of Michigan, 4250 Plymouth Road, Ann Arbor, MI 48105, USA. Email: sooeunc@med.umich.edu (Soo-Eun Chang)

Inferior frontal cortex pars opercularis (IFCop) features a distinct cerebral dominance and vast functional heterogeneity. Left and right IFCop are implicated in developmental stuttering. Weak left IFCop connections and divergent connectivity of hyperactive right IFCop regions have been related to impeded speech. Here, we reanalyzed diffusion magnetic resonance imaging data from 83 children (41 stuttering). We generated connection probability maps of functionally segregated area 44 parcels and calculated hemisphere-wise analyses of variance. Children who stutter showed reduced connectivity of executive, rostral-motor, and caudal-motor corticostriatal projections from the left IFCop. We discuss this finding in the context of tracing studies from the macaque area 44, which leads to the need to reconsider current models of speech motor control. Unlike the left, the right IFCop revealed increased connectivity of the inferior posterior ventral parcel and decreased connectivity of the posterior dorsal parcel with the anterior insula, particularly in stuttering boys. This divergent connectivity pattern in young children adds to the debate on potential core deficits in stuttering and challenges the theory that right hemisphere differences might exclusively indicate compensatory changes that evolve from lifelong exposure. Instead, early right prefrontal connectivity differences may reflect additional brain signatures of aberrant cognition–emotion–action influencing speech motor control.

Key words: stuttering; diffusion-weighted imaging; probabilistic tractography; inferior frontal gyrus pars opercularis; basal ganglia thalamocortical circuitry.

Introduction

Developmental stuttering affects 5–8% of children and persists throughout the lifetime in approximately 1% of adults (Månsson 2000; Reilly et al. 2009; Yairi and Ambrose 2013). Males and children with a family history are more likely to persist (Singer et al. 2020), though other risk factors such as early language and speech sound development have also been suggested to predict persistent stuttering (Singer et al. 2020; Walsh et al. 2021). Characteristic stuttering symptoms include sound and syllable repetitions, involuntary speech blocks, and sound prolongations (Bloodstein and Ratner 2008). These disfluencies can be accompanied by physical concomitants such as eye-blinking and facial grimacing and covert symptoms such as physical tension or negative thoughts, feelings, and self-image. Ultimately, stuttering may adversely impact well-being and overall mental health to compromise the quality of life (Yaruss and Quesal 2006, 2014; Koedoot et al. 2011).

Knowing the neural architecture of stuttering is key to understanding how and when stuttering occurs, determining the risk for persistence, developing more targeted therapies, and informing theories and models on the neural control of speech. In the past 2 decades, considerable research efforts have begun to give insights into altered brain structures and functions in stuttering. Brain morphometry studies examining

adults who stutter have linked stuttering with abnormal gray matter in the striatum and the inferior frontal gyrus (Lu, Peng, et al. 2010; Sowman et al. 2017; Neef, Bütfering, et al. 2018; Montag et al. 2019), and white matter differences in the vicinity of the left ventral precentral cortex and rolandic operculum, and the arcuate fasciculus (AF), superior longitudinal fasciculus (SLF), frontal aslant tract (FAT), corticospinal tract, and cerebellar peduncles (Sommer et al. 2002; Jäncke et al. 2004; Watkins et al. 2008; Cykowski et al. 2010; Kronfeld-Duenias et al. 2016a, 2016b, 2018; Neef et al. 2018; Jossinger et al. 2021). Given the large-scale involvement of speech-related brain structures in stuttering, it is not surprising that further connectivity studies have reported irregular structural (Cai et al. 2014) and functional neural networks (Lu, Peng, et al. 2010; Chang et al. 2011; Neef et al. 2016; Yang et al. 2016; Kell et al. 2018; Metzger et al. 2018). However, all participants of these studies were tested years, if not decades, post-stuttering onset, complicating efforts to disentangle causes versus consequences of stuttering.

More recently, findings from longitudinal magnetic resonance imaging (MRI) studies of children who stutter (CWS) have provided support for the reported speech-dominant left hemisphere deficits in adults, pointing in particular to speech motor control regions including the left ventral motor and premotor cortex, inferior frontal cortex (IFC), supplementary motor area (SMA) and

putamen, and connecting white matter structures (Chang and Zhu 2013; Chang et al. 2015; Garnett et al. 2018). The neural circuits found to differentiate stuttering speakers to age matched controls include those linked to neural systems of speech learning (Loh et al. 2020), speech planning and selection (Bohland et al. 2010), speech initiation and timing (Schwartze et al. 2012; Dick et al. 2018; Chang and Guenther 2020), and speech auditory-motor processing (Max et al. 2004; Hickok et al. 2011).

The above speech functions arise from the distributed activity of distinct networks, with the left IFC pars opercularis (IFCop) being part of each of these networks. The IFCop occupies the posterior portion of the inferior frontal gyrus and is bordered by the inferior frontal sulcus, the lateral fissure, the anterior ascending ramus of the lateral fissure, and the inferior precentral sulcus (Amunts et al. 1999), macro-anatomical landmarks that roughly correspond to the cytoarchitectonic boundaries of area 44 (Zilles and Amunts 2018). Resting-state functional MRI (fMRI) studies suggest that area 44 has functional connectivity with: (1) the supramarginal gyrus (SMG), the caudalmost part of the superior temporal gyrus (STG) and the adjacent section of the superior temporal sulcus (STS) in the parietal and the temporal lobe, (2) the middle frontal gyrus area that harbors area 9/46v, anterior portion of the SMA, preSMA and midcingulate cortex (MCC) in the frontal lobe, and (3) the pars opercularis homolog in the contralateral hemisphere (e.g. Margulies and Petrides 2013). Major connecting fiber bundles involve the SLF and AF that connect frontal and parietotemporal regions (Catani et al. 2005; Catani and Mesulam 2008), and the FAT, which interconnects inferior frontal and superior frontal regions (Catani et al. 2013) Furthermore, corticostriatal connections between IFCop and putamen and between IFCop and caudate nucleus were suggested by a functional parcellation of the striatum using diffusion-weighted MRI and probabilistic tractography (Tziortzi et al. 2014) and by residual bootstrap Q-ball tractography (Mandelli et al. 2014). All these structural connections were validated in nonhuman primates: corticocortical, transcallosal, and corticostriatal connections were corroborated in macaque monkeys with autoradiographic tract-tracing that enables the precise designation of the termination of axons (Petrides and Pandya 2009; Korponay et al. 2020). Accordingly, in humans, core neural cortical and subcortical areas that have been reported to differ in stuttering form connections with the IFCop.

Cytoarchitectonic area 44, as described by Brodmann (1909), is connected with distributed cortical and subcortical structures and builds various functionally segregated circuits. It can be subdivided into smaller subunits according to distinctive myeloarchitectonic (Vogt 1910) and receptor architectonic features (Zilles et al. 2015) as well as functional neuroimaging studies (Clos et al. 2013; Hartwigsen et al. 2019). Specifically, anatomists subdivide area 44 myeloarchitectonically into the bistriate area 56 and the unistriate area 57 (Vogt 1910). Based on the distribution of neuroreceptor transmitters, area 44 is subdivided into a dorsal and a ventral part and has been reported to show a left-larger-than-right asymmetry of the cholinergic M2 receptor (Amunts et al. 2010). Since architectonic areas differ in connections and physiology, they likely serve different functions (Geschwind and Galaburda 1985), an assumption, supported by a recent coactivation-based parcellation of area 44. The parcellation was based on thousands of task-based functional MRI studies and revealed an even deeper subdivision into five functionally segregated subunits and circuits (Clos et al. 2013). Parceled subunits were assigned to different domain-general cognitive functions such as action imagination, working memory, or conflict resolution, and to particular speech

and language functions such as phonology, semantics, syntax, and speech. A similar coactivation-based parcellation of the right hemisphere homolog revealed functional subunits and circuits assigned to action, action inhibition, and visuospatial attention (Hartwigsen et al. 2019). Another study investigated the laterality of resting-state functional connectivity between frontal cortical areas and the striatum. This study identified three striatal regions with asymmetric corticostriatal connectivity, the left rostral central caudate, the right rostral ventral putamen, and the right caudal ventral putamen (Korponay et al. 2021). Most importantly, area 44 was the only frontal lobe region forming lateralized functional connectivity with all 3 striatal laterality hotspots. Furthermore, while language scores scaled with leftward area 44-to-caudate connectivity, response inhibition scores scaled with rightward area 44-to-putamen connectivity. Thus, left and right area 44 comprise distinct subdivisions and exhibit pronounced functional asymmetry.

While stuttering has repeatedly been linked to compromised left hemisphere speech-related structures and networks, with the left IFG being commonly reported across multiple studies corroborated through various neuroimaging methods (Watkins et al. 2008; Chang et al. 2009, 2011; Kell et al. 2009; Desai et al. 2017; Garnett et al. 2018; Thompson-Lake et al. 2022, among others), studies have only recently started to disentangle the multifaceted role of the left IFCop (Neef et al. 2016). Moreover, to date, systematic studies on the role of the right IFC in stuttering are largely lacking, despite early observations of right-shifted activity in the frontal and rolandic operculum and the anterior insula during speech tasks (Fox et al. 1996; Brown et al. 2005), and right-shifted activity in IFCop during imagined speaking (Neef et al. 2018). Although such a right shift is missing in electrophysiological recordings prior to speaking (Salmelin et al. 2000; Jenson et al. 2018, 2020), transcranial magnetic stimulation (TMS) replicated the altered cerebral lateralization in resting-state electroencephalography (EEG) activity (Busan et al. 2019). Specifically, Busan et al. (2019) recorded EEG activity while applying single TMS pulses to the SMA. Early post-TMS EEG activity was reduced in the bilateral SMA, left precentral and right parietal regions in adults who stutter compared with fluent controls. Contrastingly, later post-TMS EEG activity was increased in right temporal and right frontal regions. Reduced spreading of activation to the left premotor cortex implies a disconnection from speech motor control sites, and the later-evolving hyperconnectivity with right temporal and frontal regions together demonstrate the spatio-temporal pattern of jeopardized network dynamics. Interestingly, neuroimaging and TMS–EEG findings align with diffusion MRI data on right IFCop connectivity. Individuals with more severe stuttering had stronger right IFCop connectivity, whereas individuals with mild stuttering had a weaker right IFCop connectivity (Neef et al. 2018). Still, the role of right hemisphere IFCop alterations is less clear. Early interpretations suggest a right hemisphere compensation for compromised left hemisphere speech networks (Preibisch et al. 2003; Kell et al. 2009), while more recent studies start discussing a potential causal role (Neef et al. 2016; Neef et al. 2018) and link right hemisphere activity to sensorimotor components of speech motor control (Jenson et al. 2018).

In the current study, we reanalyzed diffusion MRI data of CWS and matched fluent peers to dissect the structural connectivity of left and right IFCop. Earlier analyses of an overlapping sample revealed that the left IFCop had attenuated structural connectivity with the left posterior parietal and temporal areas, insula, putamen, and extreme capsule in stuttering children compared to controls (Chang and Zhu 2013). The right IFCop showed a similar

pattern with weaker connections with the right superior frontal gyrus, insula, and putamen. Furthermore, fractional anisotropy, a measure of white matter integrity, in white matter underneath the left IFCop did not show the typical developmental trajectory of age-related increases as typically observed in fluently speaking peers, and fractional anisotropy correlated negatively with stuttering severity (SSI-4 score) in stuttering boys but not girls (Chang et al. 2015). Another study examining whole-brain fractional anisotropy reported significant group differences in white matter voxels along the left AF, particularly along areas underlying the temporoparietal junction and sections of the corpus callosum (Chow and Chang 2017). Group differences were also found in frontal areas near IFCop, but these effects were not as significant, possibly due to the effects of multiple crossing fibers in this area that influence the measurement of fractional anisotropy. A limitation of the above-mentioned earlier studies is that none distinguished between functional subunits within the IFCop. Examining the connectivity of subunits of the IFCop could provide insights into functionally segregated networks and circuits to enable a fine-grained investigation of functional network alterations in stuttering. Hence, in this study, we leveraged recently published maps of functionally defined subsections (parcels) of the IFCop, to compare structural connectivity of the left and right IFCop in CWS and age-matched controls. We expected that examining the structural connectivity of the IFCop to subsections would allow a more detailed investigation of specific tracts that are altered in stuttering. Guided by past findings, we hypothesized that CWS exhibit decreased connectivity involving the left IFCop relative to controls, particularly for connections of the subsections linked to phonology/overt speech (Walsh et al. 2021) as well as rhythmic sequencing (Wieland et al. 2015; Chang et al. 2016). For right IFCop, we hypothesized that CWS may exhibit greater connectivity involving parcels linked to somatomotor and action inhibition functions (Neef et al. 2018). We further sought to explore whether any observed structural connectivity differences in CWS would be modulated by age, sex, and stuttering severity.

Material and methods
Participants

A total of 83 children (41 stuttering, 26 boys; 42 controls, 21 boys) between 3 and 11 years of age participated. All were monolingual native North American English speakers without concomitant developmental disorders, including dyslexia, attention deficit hyperactivity disorder (ADHD), learning delay, psychiatric conditions. All participants were recruited as part of a larger longitudinal study where children made yearly visits, up to 3 or 4 times. Because of this, we were able to track whether each child had gone on to receive a diagnosis for any other comorbid neurodevelopmental condition, including ADHD. Thus, although the inclusion criteria for initial recruitment specified that no other neurodevelopmental condition was present, some of the children did go on to receive another diagnosis in later years. Among the 83 children whose data were included in this study, 1 control child and 2 CWS reported receiving an ADHD diagnosis, and 1 stuttering child received an attention deficit disorder diagnosis. All children underwent careful screening to ensure normal speech and language developmental history except for the presence of stuttering in the experimental groups. The CWS and controls were matched in age, handedness (Oldfield 1971), and socioeconomic status (Hollingshead 1975). While most participants were strongly right-handed, 6 children were left-handed (3 stuttering, 3 control) and 7 ambidextrous (5 stuttering, 2 control). All participants were tested on a battery of standardized speech,

language, and cognitive tests, audiometric hearing screening, oral-motor screening, and cognitive evaluations. Details on behavioral testing procedures can be found in our previous publications (Chang and Zhu 2013; Chang et al. 2015; Chow and Chang 2017). In brief, a licensed and certified Speech-Language Pathologist (hereafter, SLP), administered all tests, including standardized speech, language, and cognitive assessments: the Peabody Picture Vocabulary Test (PPVT-3; Dunn and Dunn 2007), Expressive Vocabulary Test (EVT-2; Williams 2007), Goldman-Fristoe Test of Articulation (GFTA-2; Goldman 2000), Wechsler Preschool and Primary Scale of Intelligence (WPPSI-III; for children 2: 6–7:3; Wechsler 2002), and Wechsler Abbreviated Scale of Intelligence (WASI; for children aged 7 and up; Wechsler 1999). Children were excluded if scores fell below 2 standard deviations (SD) of the mean on any of the standardized assessments. The average test scores for each group are listed in Table 1.

Stuttering severity was assessed by collecting samples of spontaneous speech elicited through storytelling and conversational tasks with a parent and the SLP. These samples were video-recorded for further offline analyses. We calculated percent stuttered utterances per number of syllables based on narrative samples containing a conversation with the clinician and a monologue elicited with storytelling with a pictures-only book ("Frog, where are you?"; Mayer 1969). In addition, the Stuttering Severity Instrument (SSI; Riley 2009) was used to examine the frequency and duration of disfluencies occurring in the speech samp and any physical concomitants associated with stuttering; all of these measures were incorporated into a composite stuttering severity rating. To determine the measurement reliability of the SSI score, an intraclass correlation coefficient was calculated based on the ratings from 2 independent SLPs with substantial clinical experience in stuttering on children's speech samples. All CWS were diagnosed with stuttering at the initial visit. The criteria to be considered stuttering included scoring at 10 or above (very mild or higher) on the composite SSI score, and percent occurrence of stuttering (%SLD) at or higher than 3%. In some cases, children whose scores fell below this range were still considered stuttering if the instances of observed stuttering were qualitatively consistent with those observed in developmental stuttering as assessed by the SLP, and with parent confirmation and expressed concern about their child's fluency. For controls, the inclusion criteria included never having been diagnosed with stuttering, no family history of stuttering, lack of parental concern for their child's speech fluency, with %SLD < 3%.

In addition to the speech-language and cognitive tests, all children went through mock scanning during a separate visit to get familiarized with the scanner environment and procedures and to practice keeping still while lying inside the bore for stretches of time. Recordings of MRI noise were played during this session so that children were aware that they would hear loud sounds during scanning. This session was repeated in some children as needed. All children were paid a nominal remuneration and were given small prizes (e.g. stickers) for their participation. All procedures used in this study were approved by the Michigan State University Institutional Review Board. All parents signed a written informed consent form and all children provided either a verbal assent (non-readers) or signed an assent form (readers). An overlapping sample of diffusion tensor imaging (DTI) data was reported in other studies (see Supplementary Tables S1–S4).

MRI acquisition

MRI scans were acquired on a GE 3 T SignaVR HDx MR scanner (GE Healthcare) with an 8-channel head coil. During each session, 180 T1-weighted 1-mm^3 isotropic volumetric inversion recovery

Table 1. Subject demographic information.

	Controls N = 42 (21 boys)		Children who stutter N = 41 (26 boys)		Test (*df*) 1.72[a]	P 0.270
	Mean (SD)	Range	Mean (SD)	Range		
Age (years)	6.52 (2.04)	3.25–10.75	6.29 (2.08)	3.08–11.00	0.53 (80.85)	0.601
Maternal education	6.37 (0.62)	5–7	6.24 (0.77)	4–7	0.80 (76.53)	0.427
Full-scale IQ[a]	114.68 (14.3)	84–144	105.90 (14.6)	81– 138	2.77 (80.88)	0.007
Performance IQ	111.59 (15.9)	77–145	105.85 (13.9)	79– 135	1.75 (80.05)	0.084
Verbal IQ[a]	117.05 (14.9)	87–153	105.54 (14.2)	77– 137	3.60 (80.95)	0.001
PPVT[b]	118.26 (13.6)	95–151	110.07 (13.2)	86– 147	2.78 (80.99)	0.007
EVT[b]	115.66 (14.3)	90–149	106.66 (12.3)	87—137	3.08 (79.63)	0.003
GFTA	105.31 (7.96)	81–123	103.61 (8.8)	77—121	0.92 (79.78)	0.359
%SLD[c]	1.08 (0.88)	0.0–3.24	6.17 (5.8)	0.2–30.2	−5.56 (41.84)	0.000
%OD	4.94 (2.68)	0.0–10.85	5.29 (2.7)	1.0–12.7	−0.60 (80.00)	0.548
SSI-4 at the initial visit	N/A	N/A	19.54 (8.01)	6–48		

[a]Independent samples *t*-test. [b]Controls exhibited a significantly higher score than the stuttering group. [c]CWS exhibited a significantly higher score than the control group.

fast spoiled gradient-recalled images, with cerebrospinal fluid suppressed, were obtained to cover the whole brain (echo time [TE] = 3.8 ms, time of repetition [TR] = 8.6 ms, time of inversion 831 ms, repetition time of inversion 2332 ms, flip angle 8°, and receiver bandwidth ± 20.8 kHz). After the T1 data acquisition, first and high-order shimming procedures were carried out to improve magnetic field homogeneity. The DTI data were acquired with a dual spin-echo echo-planar imaging sequence with 48 contiguous 2.4-mm axial slices in an interleaved order, field of view 22 x 22 cm, matrix size 128 x 128, number of excitations = 2, TE = 77.5 ms, TR = 13.7 s, 25 diffusion-weighted volumes with b = 1,000 s/mm^2, one volume with b = 0 and parallel imaging acceleration factor = 2. DTI acquisition lasted for 12 min and 6 s. One staff member sat inside the scanner room next to the child to monitor the child's comfort and ensure cooperation during scanning. During the acquisition of volumetric T1-weighted scans and DTI scans, the children viewed a movie to help them stay still.

Preprocessing of diffusion data

Prior to preprocessing, diffusion-weighted MRI data were inspected for motion artifacts, signal drop-outs, poor signal-to-noise ratio, and image artifacts (Chang et al. 2015). Preprocessing was performed using FMRIB's diffusion toolbox (FSL v6.0.0, https://fsl.fmrib.ox.ac.uk) as well as MRtrix3 (https://www.mrtrix.org/). Data were first denoised with dwidenoise and mrdegibbs from MRtrix. Data were then corrected for motion and eddy currents, including outlier replacement (Andersson et al. 2016; Andersson and Sotiropoulos 2016). Automated quality control was run using FSL's eddy_quad and eddy_squad programs.

ROI definition

As displayed in Figure 1, we selected 8 regions of interest (ROI)s, 5 in the left IFCop and 3 in the right IFCop to serve as seed masks for the probabilistic fiber tracking. All seed masks were derived from previous coactivation-based parcellation studies of left area 44 (Clos et al. 2013) and right areas 44 and 45 (Hartwigsen et al. 2019). Accordingly, left area 44 was split into an anterior dorsal (ad), posterior dorsal (pd), anterior ventral (av), posterior ventral (pv), and inferior frontal junction (ifj) mask. Because the left hemisphere parcellation was limited to area 44 (Clos et al. 2013), we restricted the probabilistic tracking in the right hemisphere to three parcels that fell within right area 44 voxels, a posterior
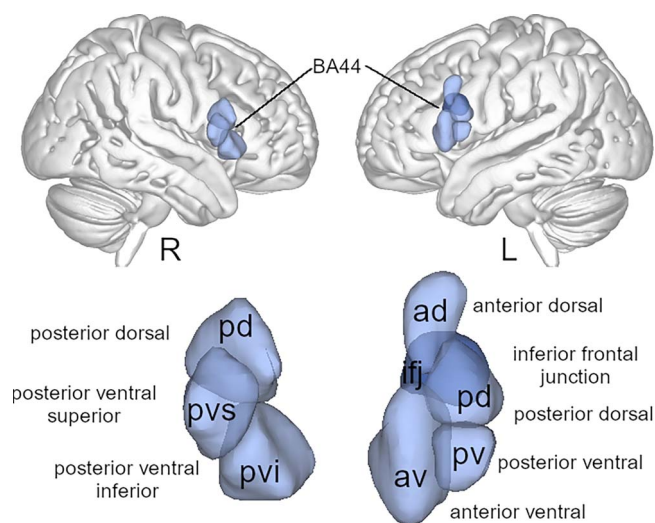

Fig. 1. Seed ROIs for probabilistic tractography. Brodmann area 44; (BA44, Clos et al. 2013; Hartwigsen et al. 2019).

dorsal (pd), posterior ventral superior (pvs), and posterior ventral inferior (pvi) mask (Hartwigsen et al. 2019).

Previous coactivation-based parcellations were calculated on maximum probability maps derived from the cytoarchitectonic mapping of 10 postmortem human brains (Amunts et al. 1999), registered to the 3D coordinate system of the Montreal Neurological Institute and Hospital (MNI) space (Amunts et al. 2004; Evans et al. 2012). Probability maps specify the likelihood that a particular voxel in the template brain belongs to the cytoarchitectonically specified Brodmann area (Brodmann 1909). This mapping procedure revealed that area 44 primarily occupies the pars opercularis of the inferior frontal gyrus. However, cytoarchitectonic borders do not consistently coincide with sulcal contours (Amunts et al. 1999), and rami and sulci of this frontal region are highly variable, making it difficult to reliably define the border between area 44 with neighboring areas 45 (anteriorly), 6 (posteriorly), ifs/ifj (dorsally), and op8 (ventrally) (Zilles and Amunts 2018).

A reliable definition of functionally distinct cortical areas is important to draw reliable inferences from neuroimaging data. Therefore, the functional segregation of left and right area 44 probability maps via dissociative network activity likely reflects operative subunits of this heterogeneous cortical region.

According to the coactivation-based parcellation, the functional segregation of the left IFCop links posterior parcels with action processes, i.e. rhythmic sequencing (pv) and phonology and overt speech (pd). Anterior parcels were associated with language and cognition, i.e. detection of meaning (av), working memory (ad), and task switching/cognitive control (ifj) (Clos et al. 2013). Unlike the left, right IFGop parcels were not associated with speech and language functions. Posterior ventral parcels were associated with action imagination and execution (pvs) and action inhibition (pvi), and a posterior dorsal parcel (pd) was associated with spatial attention (Hartwigsen et al. 2019).

Seed masks were transformed from the MNI space to the individual's native DTI space. First, a subject's anatomical image was coregistered to their b0 image. Then the anatomical image was registered to MNI space using the CAT12 and DARTEL toolboxes of SPM. This resulted in normal and inverse warp transformations. The inverse transformations were used to warp the MNI space masks into each individual subject's native DTI space.

Probabilistic tractography

In preparation for probabilistic tracking, we computed the fiber orientation distribution for every voxel with FSL's CUDA enabled BEDPOSTX (Behrens et al. 2007) software. Up to 3 fiber orientations were modeled in each voxel, which was used for the computation of tracking directions. Probabilistic tracking was performed unidirectionally from each of the 8 seed ROIs separately for every participant. No target, waypoint, or exclusion masks were included. We used FSL CUDA enabled PROBTRACKX2 (Behrens et al. 2007) with 1,000,000 sample tracts per seed voxel and otherwise default parameters (step length of 0.5 mm, curvature threshold of 0.2, maximum of 2,000 steps per streamline, volume fraction threshold of subsidiary fiber orientations of 0.01). As the range of PROBTRACKX output images covered several orders of magnitude, we applied a logarithmic transform to each of the resulting tractography visitation maps to reduce the dynamic range. The transformed maps were then scaled with the log of the total number of streamlines as a function of the seed ROI's size to account for ROI size differences between participants (Neef et al. 2018; Finkl et al. 2019). The resultant individual maps were normalized to the FSL-FA template in MNI space (1 mm isotropic) using the warps calculated on the subjects' anatomical images. The maps were then submitted to permutation analysis of linear models (PALM; Winkler et al. 2014). Apart from the normalization process, which implies a certain degree of smoothing, tractography images were not additionally smoothed.

Statistical analyses

Each voxel of an individual probabilistic fiber tracking map carries information of the likelihood of sharing structural connections with the region in the seed mask, given as the number of streamlines. This artificial measure is a proxy estimation of white matter connectivity and reflects the coherence of the underlying white matter structure. We fed normalized connectivity maps into PALM and tested 2 ANOVA models (Winkler et al. 2014), one for each hemisphere. Both models had group as a between-subjects factor and ROI as a repeated measures within-subjects factor. We calculated contrasts for the main effect of group, the main effect of ROI, and the interaction of Group × ROI. We masked out areas with low or improbable connectivity values. To create the exclusion mask, we calculated an average-scaled and normalized tractogram of all subjects in MNI-space and masked out regions with values lower than 0.2. All results were obtained using an uncorrected *P*-value of 0.005 at voxel level, a family-wise error (FWE) corrected

P-value of 0.05 at cluster level. For the left hemisphere, contrasts were calculated with *n* = 415 (83 individual maps multiplied by 5 seed masks). Dataset from 1 stuttering boy was excluded because the mean cluster connectivity value in 4 out of 5 left IFCop fell below 0.1. The right hemisphere data for this child were retained. In the right hemisphere, contrasts were calculated with *n* = 249 (83 individual maps multiplied by 3 seed masks). In the following, we use "mean ± SD" for reporting mean and standard deviation.

Post hoc analyses

Significant clusters were further investigated in R (version 4.1.2) to test the influence of covariates and to scrutinize significant interactions and effects. Therefore, we extracted the mean connectivity from respective clusters for every participant and fitted respective mixed-effects models to the mean connectivity to emulate the effect found with PALM. Subsequently, we added step by step variables to the model to explore whether they had a significant impact on the model fit. Verbal IQ was first added to the model to account for differences between groups. Age and sex and respective interactions were subsequently added to test potential maturational influences. Furthermore, we added the 3-way interaction age × group × sex to test whether the effect of the group was modulated by age or sex. Finally, we tested the 3-way interaction sex × group × ROI to test whether sex influences the group × ROI interaction. Eventually, we used the ANOVA function in R, which implements a sequential sum of squares (type I). R-code and data are provided under https://owncloud.gwdg.de/index.php/s/I4maQMqFZBv5BIO. For the statistical comparisons of the fits, the alpha level was adjusted with the Bonferroni-Holm method. To determine the direction of main effects and interactions, we calculated post hoc *t*-tests. Between-group differences were further characterized with the effect size *r*.

Finally, we tested whether stuttering severity (SSI total scores) was related to connectivity in any of the significant clusters in CWS. Therefore, we fitted further mixed-effects models to the extracted mean connectivity data. The baseline model included the variables verbal IQ, age, sex, ROI, and the sex × ROI interaction with subject and ROI as random effects. We tested whether the model fit improved by including SSI, SSI × ROI, SSI × sex, and SSI × ROI × sex.

Because mixed-effects models were calculated for every significant cluster in PALM, we adjusted the alpha level across clusters with a Bonferroni correction, i.e. *P* < 0.017 (0.05/3).

Data availability

The data that support the findings of this study are available from S.-E.C. (sooeunc@med.umich.edu) upon reasonable request.

Results
Behavioral assessments

The children with stuttering and controls did not differ in age or socioeconomic status as assessed through maternal education (Table 1). The control group scored significantly higher than the persistent on verbal IQ [*t*(80.95) = 3.60, *P* = 0.001, *r* = 0.37] and full IQ [*t*(80.88) = 2.77, *P* = 0.007, *r* = 0.29], while the groups did not differ on the performance IQ measure [*t*(80.05) = 1.75, *P* = 0.09, *r* = 0.19]. The stuttering group furthermore scored significantly lower than controls on the vocabulary tests PPVT [*t*(80.99) = 2.78, *P* = 0.007, *r* = 0.30] and EVT [*t*(79.63) = 3.08, *P* = 0.003, *r* = 0.33]. The stuttering group exhibited significantly higher %SLDs than controls [*t*(41.84) = −5.56, *P* < 0.001, *r* = 0.65], while the 2 groups did not differ in the frequency of other disfluencies (%OD)
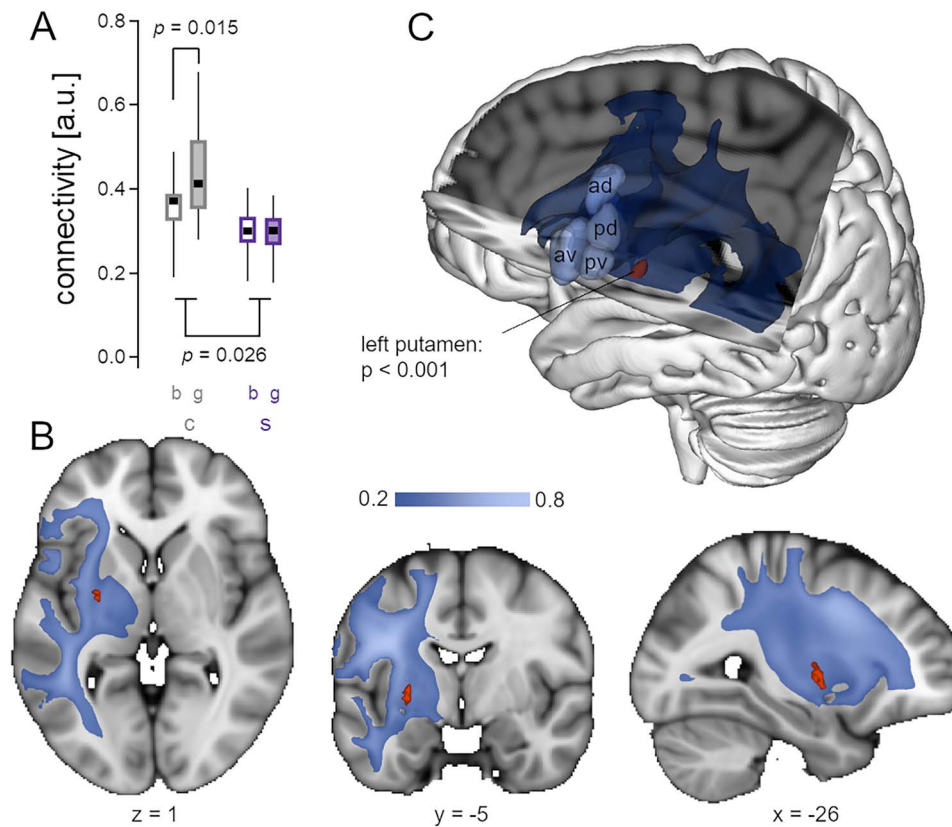
Fig. 2. Tractography results with seed volumes in left IFCop area 44. (A) The boxplot displays the mean logarithmized connectivity. CWS have reduced structural connectivity in the putamen compared to fluent peers, independent of the seed volume in the IFCop, area 44. Girls in the control group had higher IFCop-to-putamen connectivity than boys. (B) The 2D-slices indicate the tractogram threshold at 0.2 as used for statistical testing. Red indicates significant voxels. Coordinates are given in MNI-space. (C) For visualization purposes, the tractogram in the 3D image is presented at a threshold of 0.4. Abbreviations: Ad, anterior dorsal; av, anterior ventral; pd, posterior dorsal; pv, posterior ventral; s, children who stutter; c, controls.

$[t(80.00) = -0.60, P = 0.55, r = 0.07]$. Because significant group differences were observed in Verbal IQ, we entered Verbal IQ as a first covariate in subsequent mixed-effects analyses. Though PPVT and EVT also differed between groups, these were not additionally entered as covariates to avoid multicollinearity, given that verbal IQ is highly correlated with both PPVT (Krasileva et al. 2017) and EVT scores (Gilmore et al. 2018).

Structural connectivity of the left IFCop

Left IFCop connectivity analysis with PALM revealed an effect of group (Fig. 2A, Table 2), but no effect of ROI, and no group × ROI interaction. Post hoc group comparisons indicated that CWS have lower connectivity than controls $[M_{CWS} = 0.30 \pm 0.06;$ $M_{Controls} = 0.39 \pm 0.10, t(66.4) = 4.98, P < 0.0001, r = 0.52]$. The significant cluster was located in the left putamen including voxels of the caudal-motor, rostral-motor, and executive subregion (Tziortzi et al. 2014).

Post hoc mixed-effects model analyses revealed a significant sex effect (Table 3): boys exhibited lower connectivity than girls $[M_{boy} = 0.33 \pm 0.07; M_{girls} = 0.38 \pm 0.11, t(58.9) = 2.28, P = 0.026, r = 0.28]$. There was furthermore a sex × group interaction (Table 3) indicating that control girls have higher left IFCop connectivity $(M_{girls} = 0.43 \pm 0.11)$ than control boys $[M_{boys} = 0.35 \pm 0.08, t(37.4) = 2.54, P = 0.015, r = 0.38]$, whereas stuttering girls have low connectivity $(M_{girls} = 0.30 \pm 0.06)$ similar to stuttering boys $(M_{boys} = 0.30 \pm 0.06, $ Fig. 2B).

Structural connectivity of the right IFCop

Right IFCop connectivity analysis produced one large cluster for the effect of ROI (Table 2) and one different cluster for the interaction between group and ROI (Table 2). There was no significant cluster for an effect of group.

The effect of ROI indicated that the 3 seed masks in the right IFCop have different connection probabilities in a white matter region that was located laterally and involved voxels of the AF, SLF, and FAT (Fig. 3A). Post hoc t-tests indicated higher connectivity of the pvs subregion than pvi and pd. Post hoc mixed-effects model comparisons yielded significant interactions of group × sex × ROI and of group × sex (Table 3). Stuttering girls had a lower right IFCop connectivity than stuttering boys $[M_{girls} = 0.50 \pm 0.06; M_{boys} = 0.54 \pm 0.03; t(17.7) = -2.7, P = 0.015, r = 0.54]$, whereas control girls had a similar connectivity comparable to control boys $[M_{girls} = 0.53 \pm 0.30; M_{boys} = 0.51 \pm 0.37; t(29.4) = 1.4, P = 0.175, r = 0.25]$. This sex difference was significant for pvs connections in CWS $[M_{girls} = 0.49 \pm 0.09; M_{boys} = 0.59 \pm 0.03; t(16.68) = -4.42, P = 0.0004, r = 0.73]$, and marginal in pvi connections in CWS $[M_{girls} = 0.51 \pm 0.10; M_{boys} = 0.56 \pm 0.05; t(17.83) = -1.9, P = 0.079, r = 0.40]$. Furthermore, stuttering boys had significantly higher pvs and pvi connectivity than control boys (Fig. 3B).

The group × ROI interaction was located in white matter voxels in the vicinity of the right insula, frontal operculum, and IFC pars triangularis, and included voxels of the FAT, SLF, and AF according to the XTRACT HCP Probabilistic Tract Atlases (Warrington et al. 2020, Fig. 3C). In this medial anterior region, IFCop

Table 2. Locations of significant clusters of different IFCop connectivity.

Brain area	x	y	z	Volume (mm³)	Z
Effect of group (left IFCop)					
L Putamen	−24.5	−6	4.5	152	3.75
Effect of ROI (right IFCop)					
R Arcuate fasciculus/R Superior longitudinal fasciculus	35.8	3.0	18.1	16,136	4.06
Group × ROI interaction (right IFCop)					
R Vicinity of the right insula	31.4	20.7	4.2	1,046	1.81
R Frontal operculum	37.5	22.2	7.3		
R IFG pars triangularis	55.5	27	0		

Thresholded at $P < 0.05$. Peak coordinates are provided in MNI152 space. The extent of each cluster is provided in voxels. The Z-value for the center of gravity voxel is shown in the final column.

Table 3. Post hoc mixed-effects model analyses for all participants.

	Left IFCop[a] Effect of group		Right IFCop Effect of ROI		Right IFCop Group × ROI	
	χ^2(df)	P	χ^2(df)	P	χ^2(df)	P
Emulated PALM						
Group	**21.64 (5)**	**<0.0001**	0.31 (5)	0.575	1.77 (5)	0.183
ROI	2.75 (9)	0.600	**16.57 (7)**	**0.003**	**12.922 (7)**	**0.002**
Group × ROI	5.04 (13)	0.283	6.30 (9)	0.043	**21.24 (9)**	**<0.0001**
Covariates						
+ Verbal IQ	3.42 (14)	0.064	0.16 (10)	0.686	1.08 (10)	0.299
+ Age	2.81 (15)	0.094	0.02 (11)	0.878	0.02 (11)	0.901
+ Age × Group	0.13 (16)	0.715	0.03 (12)	0.860	0.42 (12)	0.516
+ Sex	**5.33 (17)**	**0.021**	0.90 (13)	0.343	0.02 (13)	0.875
+ Sex × Group	**5.03 (18)**	**0.025**	**10.56 (14)**	**0.001**	1.67 (14)	0.196
+ Age × Group × Sex	0.38 (20)	0.826	1.99 (16)	0.369	3.17 (16)	0.205
+ Sex × Group × ROI	15.07 (28)	0.058	**12.78 (20)**	**0.013**	**21.25 (20)**	**0.0003**

[a]One CWS boy was excluded because connectivity was < 0.1. Statistically significant results are highlighted in bold.

connectivity varied with IFCop seed ROI and group. CWS showed higher connectivity of the pvi than controls ($M_{CWS} = 0.61 \pm 0.14$; $M_{Controls} = 0.48 \pm 0.15$), but marginally lower connectivity of the pd than controls ($M_{CWS} = 0.42 \pm 0.13$; $M_{Controls} = 0.50 \pm 0.16$). The connectivity of the pvs was not different between groups. Furthermore, right IFCop connectivity varied between seed ROIs in CWS, where greatest connectivity was seen for pvi, followed by pvs, then pd. Controls showed no ROI-specific connectivity differences (Fig. 3C). Post hoc mixed-effects models yielded no further effects or interactions, but an interaction of group × ROI × sex. The model fit was significantly improved by adding the interaction term [$\chi^2(20) = 21.98$, $P = 0.0002$]. This interaction reflected that stuttering boys had higher pvi connectivity than stuttering girls [$t(18.09) = −4.6$, $P = 0.0002$, $r = 0.73$] and control boys [$t(29.1) = −7.2$, $P = 6.622e-08$, $r = 0.80$], and stuttering boys had lower pd connectivity than control boys [$t(23.4) = 1.9$, $P = 0.074$, $r = 0.37$] and marginally lower connectivity than stuttering girls (Fig. 3D).

Relationship between stuttering severity and IFCop connectivity

Left IFCop connectivity with the left putamen was not influenced by stuttering severity and there was no interaction between stuttering severity, sex, and ROI (Table 4).

Right IFCop connectivity of the anterior medial cluster varied with stuttering severity depending on sex (Table 4). So, for stuttering girls, stuttering severity tended to increase with increasing connection probability. In contrast, for stuttering boys stuttering severity tended to decrease with increasing connection

probability (Fig. 3E). This pattern is reflected in the significant SSI × sex interaction [$\chi^2(15) = 6.0$, $P = 0.011$]. However, Pearson's correlations between SSI and connection probability were not significant, either for the average across pvs, pvi, and pd, or for single seed ROIs, neither for girls nor for boys.

Discussion

Robust structural connectivity of speech-related neuronal networks is essential for speech production and fluency (Sarubbo et al. 2015). As IFCop serves as an interface between speech planning and execution (Sahin et al. 2009; Flinker et al. 2015; Ferpozzi et al. 2018), is involved in fluent speech production (Long et al. 2016), and shares network connections with distant cortical and subcortical speech regions (Catani et al. 2005, 2013; Mandelli et al. 2014; Tziortzi et al. 2014), we scrutinized its structural connectivity in a large sample of CWS and fluent peers. We took advantage of recently identified subsections of the IFCop in both hemispheres, each linked to supporting distinct functions (Clos et al. 2013; Hartwigsen et al. 2019). By examining structural connectivity involving each of these subsections of IFCop, we expected to add greater granularity to previous findings of aberrant connectivity of the IFCop in stuttering speakers. Namely, previous DTI studies suggest that developmental stuttering may be caused by a disconnection of left hemisphere structures, including SLF/AF, FAT, or corticostriatal connections (Sommer et al. 2002; Watkins et al. 2008; Connally et al. 2014; Kronfeld-Duenias et al. 2016b; Chow and Chang 2017; Neef et al. 2018, among others). Unlike the left, right hemisphere
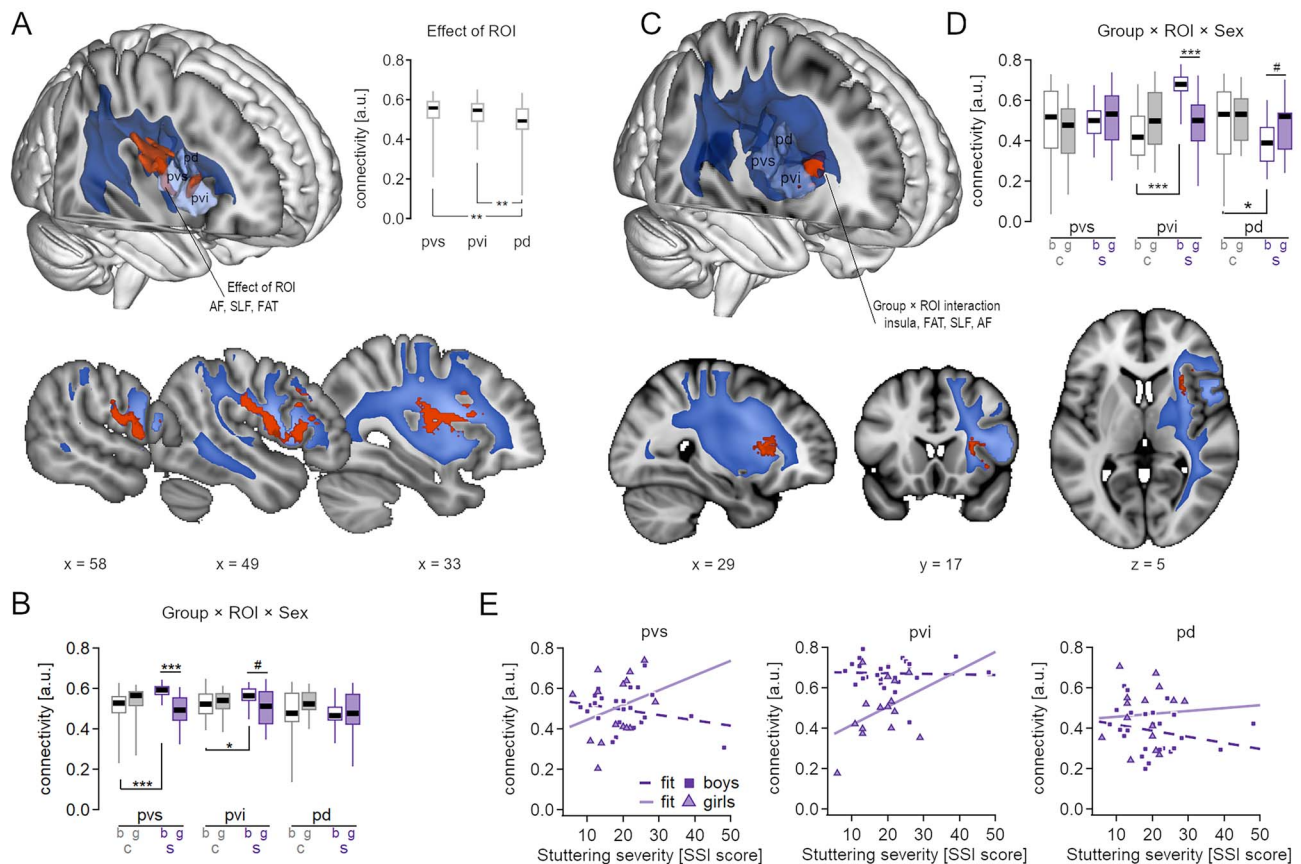
Fig. 3. Tractography results with seed volumes in right IFCop area 44. (A) One significant cluster from PALM indicates white matter with increased connection probability of pvs compared to pd and pvi. The cluster was located laterally and included fractions of AF, SLF, and FAT. (B) Post hoc mixed-effects model analyses for this lateral cluster indicated a group × ROI × sex interaction. The interaction was driven by stuttering boys who showed increased connection probability with pvs compared to stuttering girls and compared to control boys. Like pvs, pvi tended to show the same pattern. (C) The second significant cluster from PALM resulted from a group × ROI interaction. The cluster was located anterior medial in white matter in the vicinity of the insula, including FAT, SLF, and AF. Red indicates significant effects. Blue in slices ranges from 0 (no connectivity) to 1 (maximal connectivity). The tractogram threshold is 0.2, as used for statistical testing. For visualization purposes, the tractogram in 3D images is presented at a threshold of 0.4. (D) Post hoc mixed-effects model analyses for this anterior medial cluster indicated a group × ROI × sex interaction. The interaction was driven by stuttering boys who showed increased connection probability with pvi compared to stuttering girls and compared to control boys. Unlike pvi, pd tended to show the opposite pattern. Stuttering boys had a decreased connection probability compared to control boys and a trend towards decreased connection probability compared to stuttering girls. Boxplots indicate the mean logarithmized connectivity. Asterisks indicate significant t-tests with $^{\#}P < 0.1$, $^{*}P < 0.05$, $^{**}P < 0.01$, $^{***}P < 0.001$. Coordinates are given in MNI-space. (E) In stuttering girls, stuttering severity tended to increase with increasing connection probability, while stuttering boys showed the opposite effect that was reflected in a significant SSI × sex interaction [$\chi^2(14) = 6.0$, $P = 0.014$]. However, Pearson's correlations were not significant. Abbreviations: AF, arcuate fasciculus; FAT, frontal aslant tract; SLF, superior longitudinal fasciculus; pvs, posterior ventral superior; pvi, posterior ventral inferior; pd, posterior dorsal; s, children who stutter; c, controls; b, boys; g, girls.

Table 4. Influence of SSI on connectivity in CWS.

	Left IFCop[a] Effect of Group		Right IFCop Effect of ROI		Right IFCop Group × ROI	
	χ^2(df)	P	χ^2(df)	P	χ^2(df)	P
lme(Connectivity ~ 1 + ROI + Verbal IQ+ Age + Sex + Sex*ROI, random = ~ 1|Subject/ROI)						
SSI	0.02 (16)	0.879	0.05 (12)	0.827	0.17 (12)	0.678
SSI × ROI	6.51 (20)	0.164	022 (14)	0.897	0.88 (14)	0.644
SSI × Sex	0.01 (21)	0.915	1.48 (15)	0.224	6.42 (15)	**0.011**
SSI × Sex × ROI	9.49 (25)	0.050	4.10 (17)	0.129	0.97 (17)	0.617

[a]One CWS boy was excluded because connectivity was < 0.1. Statistically significant results are highlighted in bold.

findings have been inconsistent, and have suggested the presence of both hyper- and hypo-connectivity, related to compensation, maladaptation, or hyperactive inhibition in stuttering. Here, we provide further evidence for weak left IFCop corticostriatal

projections, a finding that supports the implication of cortico-basal ganglia-thalamocortical loops in developmental stuttering. Unlike the left, the different right IFCop parcels showed both increased and decreased connection probability, in particular in

boys who stutter. Whether this disproportionate involvement of right prefrontal structures in stuttering reflects causal, compensatory, maladaptive processes or their combination, remains unclear and warrants further investigation.

Children who stutter showed a reduced left IFCop-to-putamen connectivity

The structural connectivity of the left IFCop with the putamen was reduced in CWS compared to fluent peers. This finding is not new and has been reported and discussed previously for an overlapping sample of data with a different DTI analysis approach (Chang and Zhu 2013). While our reanalyzes aimed at dissociating functionally segregated structural networks, the current diffusion-based fiber tracking results in the left hemisphere do not support this presumption. However, a recent tracing study in macaque monkeys (Korponay et al. 2020), provided for the first time structural support for an assessment of corticostriatal projections of area 44 in developmental stuttering. These supporting insights from macaque area 44 were only available after the initial observation of a reduced left IFCop-to-putamen connectivity in stuttering. In the following, we discuss how these findings converge.

The putamen is part of the striatum, the primary input area of the basal ganglia. It receives input from all cortical regions, including the frontal cortex, and plays a central role in motor behavior (Selemon and Goldman-Rakic 1985; Haber 2016). Current models of speech motor control assign the putamen to a speech motor loop, which receives cortical input from the ventral premotor cortex (vPMC, Civier et al. 2013; Guenther 2016). Another input structure of the striatum, the caudate nucleus, is modeled as part of a speech planning loop, which receives cortical input from the IFCop (Civier et al. 2013; Guenther 2016). These models contrast with the tracing study in monkeys that showed that cytoarchitectonic area 44 projects to the caudate nucleus and the putamen (Korponay et al. 2020). These corticostriatal connections have a topographic organization. While projections from the rostral (anterior) area 44 terminated primarily in the caudate nucleus, projections from the caudal (posterior) area 44 terminated primarily in the putamen. The current DTI fibertracking showed no such segregated structural IFCop connectivity. But we showed a reduced IFCop-to-putamen connectivity in stuttering children, linking stuttering to an anatomical connection that has not been considered in theories and models of speech motor control.

The relation between an IFCop-putamen connection and fluent speech lends functional support to an exciting interpretation of the structural data from the tracing study. Korponay and colleagues found intermingled innervation in the striatal targets of area 44. The caudal target area also receives input from the ventral lateral prefrontal cortex and other nonmotor-related prefrontal regions, and the putaminal target area received input from five cortical regions involved in vocalization: ventral premotor area 6VR, dorsal Sylvian opercular area ProM, motor cingulate area, pre-SMA, and SMA (Loh et al. 2020). While these combinations could be expected from the proposed cognitive role of the caudate nucleus and the motor role of the putamen, the intermingled nature of the projections provides a structural basis not only for separated cortico-striatal closed loops but for input convergence and mixing in the striatum. The structural observation of projections from IFCop-putamen and 5 vocalization-related areas onto the same putaminal area together with the functional observation of stuttering under reduced IFCop-putamen connectivity makes such a local impact of IFCop on putaminal speech-motor control an attractive hypothesis. Integration of multisite input

to the putamen and local processing into speech models would facilitate future, model-driven exploration of this hypothesis.

Persistent stuttering has often been associated with neural alterations in the basal ganglia (Alm 2004; Giraud et al. 2008; Watkins et al. 2008; Lu, Peng, et al. 2010; Civier et al. 2013; Sowman et al. 2017; Metzger et al. 2018; Cler et al. 2021; Liman et al. 2021) and theoretical accounts on stuttering frequently suggest an implication of the putamen (Alm 2004, 2021; Giraud et al. 2008; Civier et al. 2013; Chang and Guenther 2020). Compared to controls, adults who stutter have an increased gray matter volume of the left putamen (Lu, Peng, et al. 2010) and quantitative MRI suggests an elevated iron concentration in the left putamen and left frontal speech motor regions (Cler et al. 2021). Earlier imaging studies with positron emission tomography showed increased dopaminergic activity in the left insula and left putamen (Wu et al. 1997), and treatment effects were related to changes in regional blood flow in the left putamen (Ingham et al. 2013), and to changes in blood oxygenation level dependent (BOLD) activity in the left putamen (Neumann et al. 2003). A previous analysis of DTI data of an overlapping sample of the current cohort of CWS and fluent peers also revealed attenuated functional and structural connectivity between left putamen and several left hemisphere cortical regions, including IFCop and SMA in CWS (Chang and Zhu 2013). The altered left frontal lobe to left putamen connectivity has been suggested to interfere with self-initiated movements and the internal generation of temporal templates for speech utterances (Alm 2004; Chang and Guenther 2020).

Recent investigations in rodents gave novel insights on the functional role of cortico-putaminal connections. The putamen is essential for procedural learning, i.e. the acquisition of motor memories (Wymbs et al. 2012), and seems to contribute to habit formation and motor control (Rueda-Orozco and Robbe 2015). Recent studies of bilaterally coordinated movements in rats suggest that the impairment of cortico-striatal connections interfered with the stability and duration of already started bilateral movements (Pimentel-Farfan et al. 2022). According to their studies (Rueda-Orozco and Robbe 2015; Pimentel-Farfan et al. 2022), the dorsolateral striatum in rats (the rodent homolog area of the human putamen) converges contextual sensorimotor and kinematic information to provide a so-called moment-to-moment control. The authors suggested, that after learning, which is during the habitual execution of motor sequences, the dorsolateral striatum continuously integrates movement-relevant information (running speed, position, and time) to constrain the execution of motor habits. Thus, it is tempting to speculate that the here observed disruption of cortico-striatal projections in CWS likely reflects a core neural deficit. Specifically, novel principle insights on the role of corticostriatal projections suggest that stuttering might result from an insufficient cortical input to putaminal neurons to integrate contextual and kinematic information necessary to secure a fluid automatized speech motor execution. The left IFCop (area 44) might thereby support the motor loop by providing contextual information about the state of phonological sequence planning, a new hypothesis converging with the idea that area 44 seems to be an ideal hub to serve as an interface between cognition and action (Amunts et al. 2010; Clos et al. 2013; Korponay et al. 2020).

Boys who stutter showed increased right pvi connectivity and decreased right pd connectivity with the right insula

For stuttering boys, we found hyper- and hypo-connectivity of right IFCop parcels mainly in the vicinity of the right insula. The

insula shares connections with multiple cortical and subcortical regions (Nieuwenhuys 2012; Uddin et al. 2017), and a tracer study in rhesus monkeys provides evidence that area 44 indeed shares anatomical connections with the insular cortex (Deacon 1992).

Functionally, the insula is involved in a vast spectrum of tasks including interoception and pain (Craig 2009), empathy (Bernhardt and Singer 2012), emotion and motivation (Cardinal et al. 2002), salience processing (Uddin 2015), somatosensation (Chikama et al. 1997), and the insula is also activated during speech and voice production (Ackermann and Riecker 2010; Oh et al. 2014). Like the cortex, the insula can be parceled into functionally segregated and functionally convergent regions. Specifically, cognitive tasks activate the anterior-dorsal insula, social–emotional tasks activate the anterior-ventral insula, olfactory-gustatory stimuli activate the central region, and sensorimotor tasks activate the mid-posterior insula (Kurth et al. 2010). Furthermore, the first four conditions cause an overlapping activation of the anterior-dorsal insula, and therefore the insula is seen as a functional hub that relays and integrates information from different functional systems (Kurth et al. 2010). Our analyses showed altered IFCop connectivity with the anterior-dorsal and anterior ventral insula, but not with the posterior insula. This finding leads to the question of whether in stuttering boys, the imbalanced right IFCop-to-insula connectivity reflects an implication of atypical cognitive, social–emotional, or executive processing.

The functional role of the insula in speech has been greatly explored via lesion-symptom mapping and intra-operative electrical stimulation and recording from eloquent sites. Stroke-induced lesions in the left anterior insula have been associated with apraxia of speech (Dronkers 1996; Ogar et al. 2006), affected fluency (Bates et al. 2003), and coordination of complex articulatory movements (Baldo et al. 2011), suggesting a role in speech motor planning. Right posterior insular lesions have been associated with dysarthria (Baier et al. 2011). Electric stimulation of bilateral insular regions in patients with focal epilepsy or low-grade glioma induced speech arrest, speech disturbances, dysarthria, and reduced voice intensity (Isnard et al. 2004; Duffau et al. 2006; Afif et al. 2010). These observations provided direct evidence for bilateral insular involvement in speech motor processing and converge with neuroimaging studies on stuttering that frequently reported an altered speaking-related involvement of the left (Watkins et al. 2008; Howell et al. 2012; Lu et al. 2016) and right anterior insula (Brown et al. 2005; Chang et al. 2009; Lu, Chen, et al. 2010). However, whether an insular involvement is critical for speech planning and complex speech articulation or has a more general role in oral-motor control, has been debated for years (Hillis et al. 2004; Fedorenko et al. 2015; Uddin et al. 2017). A recent study recorded cortical activity from multiple sites across the insula in both hemispheres during single-word articulation of varying complexity, non-speech orofacial movement, and speech listening tasks (Woolnough et al. 2019). With this technique, it was possible to precisely localize insular activity and to resolve the time course of this activity relative to actual behavior. Anterior insula electrodes showed neither pre-articulatory nor post-articulatory activity and posterior electrodes showed only post-articulatory activity. According to their findings, the authors ruled out a pre-articulatory speech preparatory role of the insula. In the same study, the authors observed involvement of the adjacent left frontal operculum prior to articulation. In the current study, the right frontal operculum showed altered connectivity with IFCop parcels. This observation returns the right shift to mind that has been associated with persistent stuttering and that has been

interpreted as a signature of compensatory mechanisms because stuttering therapy has been reported to reduce overactivity in the right frontal operculum (Preibisch et al. 2003; Kell et al. 2009; Neumann et al. 2018). However, the fact that the right frontal operculum is already involved in CWS puts such a simplified interpretation into question.

The current study showed altered structural connectivity between right area 44 and the anterior insula and the adjacent frontal operculum. Because the right IFCpvi and the right anterior-dorsal insula are both involved in the ventral attention network (Yeo et al. 2011; Hartwigsen et al. 2019; Klugah-Brown et al. 2022), one possible explanation for the here observed hyperconnectivity in stuttering boys might be an implication of cognitive control functions. This is in line with previous findings of an altered organization of intrinsic functional networks in CWS (Chang et al. 2018). Compared to their fluent peers, in CWS internetwork connectivity was increased between the ventral attention network and the default mode network, and altered between the ventral attention network and the somatomotor network, and the anterior insula was the major hub of this disturbed between-network connectivity. The authors discuss this finding in the context of the co-occurring implication of attentional processes (Riley and Riley 2000; Donaher and Richels 2012; Eggers et al. 2013) and related this finding to inefficient utilization of attention during speech motor control. Insofar, the current finding converges with this previous observation.

One previous tractography study with adults who stutter tested structural connectivity differences for a broad range of brain regions involved in speech (Cai et al. 2014). Thereby, the authors distinguished between dorsal and ventral IFCop and observed increased connectivity between the right dorsal IFCop and the right posterior insula. In contrast, connectivity between the right ventral IFCop and pdPMC, mid-PMC, and SMA was decreased in adults who stutter compared to controls (Cai et al. 2014). This earlier observation converges with the current findings in 2 points. First, subregions of the right IFCop were associated with opposing connectivity patterns in stuttering speakers, showing both strengthened and weakened connectivity. Second, a proportionally high ratio of participating males who stutter makes it likely that these previous findings were also driven by male participants.

The previous meta-analytic coactivation-based parcellation study that motivated the current analyses, associated the right IFCpvi with action inhibition (Hartwigsen et al. 2019), and further previous neuroimaging studies with adults who stutter motivated the hypothesis that stuttering might be related to hyperactive inhibition of speech motor activity via the right posterior IFCop (Neef et al. 2016; Neef et al. 2018) and via cortico-basal ganglia thalamo cortical loops with bilateral posterior IFCops (Metzger et al. 2018). And indeed, accumulating evidence points to the right IFCop as a crucial hub in a prefronto-basal ganglia–thalamocortical network for stopping actions (Aron and Poldrack 2006; Chambers et al. 2006, 2007; Hannah et al. 2020) in particular when acting together with the pre-SMA (Wessel and Aron 2017). Action inhibition also involves the anterior insula in concert with the inferior frontal junction and the right IFCop (Sebastian et al. 2016). The involvement of these prefrontal regions during stop tasks is modulated by attentional processes since it varies with varying cognitive strategies that might be applied (Sebastian et al. 2017). For example, the right IFC/anterior insula are increasingly engaged when stopping an ongoing response becomes difficult (Hughes et al. 2013; Sebastian et al. 2017). But what precisely is the relevance of action stopping in stuttering? Action stopping is mainly addressed during error correction. The

employment of correction strategies involves (1) sensorimotor feedback control, i.e. feedback of the position of articulators and current acoustic output, (2) feedforward control, i.e. generation of corrected speech motor plans, and (3) the allocation of attentional resources to these processes. Moreover, in some cases affected children start rephrasing already planned utterances to avoid certain words or speech sounds, which recruits additional cognitive resources to constantly balance what to say and what not to say. On top of these speech-related processes are the monitoring and regulation of emotional, social, and motivational aspects of the communicative situation. The present results can only provide indirect evidence for an imbalanced neural interaction between the anterior insula and right IFCop, and the multifaceted involvement of both structures in cognition and behavior complicates the search for a clear explanation. That said, the sub-parcel connectivity analyses of the right IFCop provide novel insights into how stuttering boys, who are more likely to go on to develop persistent stuttering compared to girls, show early structural connectivity differences relevant to interfacing movement inhibition and cognitive control processes. Future investigations that involve speech and non-speech movement inhibition tasks to examine functional connectivity differences between right IFC/anterior insula may be warranted to further confirm and expand on these results. If confirmed, it may suggest that aberrant connectivity affecting efficient integration of action inhibition and cognitive control processes plays a critical role in the development and maintenance of stuttering symptoms.

Boys who stutter showed increased right pvi and right pvs connectivity with the ventral sensorimotor cortex

The second significant cluster in the right hemisphere resulted from the main effect of seed ROI and indicated a differing degree of connectivity between the 3 functionally distinct IFCop parcels and the ventral sensorimotor and sensory association areas. Specifically, IFCpvs and IFCpvi exhibited stronger structural connectivity with the ventral sensorimotor cortex than IFCpd. This finding converges with the concept that pvs and pvi are both involved in action processing and thus relate to cognitive control of sensorimotor processes (Hartwigsen et al. 2019).

Post hoc mixed-effects models revealed an influence of stuttering and sex on the connectivity between IFCop and ventral sensorimotor cortices. Again stuttering boys drove the effect by showing increased pvs connectivity compared to fluent peers and stuttering girls and a similar trend for pvi connectivity. This finding raises the question of whether boys who stutter employ right IFCop-to-sensorimotor cortex connections to facilitate speech fluency or whether this strengthened connectivity interferes with speech fluency. Correlation analyses between connectivity and stuttering severity were not significant and therefore provide no hint which interpretation to favor.

Traditional models lateralize the speech sensory-motor system to the left hemisphere (Guenther 2006, 2016; Hickok and Poeppel 2007; Hickok et al. 2011). This is also supported by a TMS study probing speech motor cortex excitability during speaking. Excitability of the left ventral motor representation of the tongue, not the right, is facilitated when actual speaking compound words (Neef et al. 2015). In contrast, adults who stutter show no facilitation of the ventral motor cortex, neither during speaking (Neef et al. 2015) nor while resting (Neef et al. 2011). The reduced state-dependent excitability of the ventral motor cortex in adults who stutter could be caused by various pathophysiologies ranging from altered intracortical regulation of excitation and inhibition to altered cortico-cortical, subcortical-cortico or

transcallosal input. In this vein, one could also only speculate about potential mechanisms behind the increased connectivity between the right IFCop and ventral sensorimotor cortex. It could reflect genetically driven immature wiring, compensatory neuroplasticity in response to stuttering, or maladaptation possibly related to overactive action inhibition or overreliance on auditory or somatosensory feedback control. Although current data were derived from young CWS, all of the participants had already been stuttering for at least 6 months. For this reason, it is difficult to disentangle whether connectivity differences reflect causes or consequences of stuttering. What the current results provide are new information on early occurring connectivity differences in young CWS in the right IFCop, suggesting greater involvement of structures supporting action processing and inhibition, particularly in stuttering boys. Whether these differences link to greater persistency rates in males who stutter will need to be further investigated in future longitudinal studies.

Limitations

Unlike previous multimodal parcellations of left area 44 (Amunts et al. 2010; Clos et al. 2013), the current diffusion-based tractography from 5 functionally segregated parcels of probabilistic area 44 yielded no statistically significant difference between the connection probability patterns. This may be due to less functional differentiation of the left IFCop at the age under investigation, or a greater variability within the CWS group in this general area. Alternatively, methodological limitations may restrict the explanatory power of diffusion tensor imaging data and limit the precise definition of the human connectome. A further detailed examination into this is warranted, including a look at functional MRI data with larger samples in future studies.

Furthermore, previous coactivation-based parcellations were calculated for the Juelich probability map of area 44 (Clos et al. 2013; Hartwigsen et al. 2019). In general, the Juelich probability map reflects the high variability of the location of a cytoarchitectonic area across 10 post-mortem brain specimens. This variability is particularly pronounced at the outer borders that in the case of area 44 likely include voxels of neighboring areas such as 6 V, 8Av, 45, and portions of the insular cortex (Amunts et al. 1999; Zilles and Amunts 2018).

It is furthermore important to note the limitations in interpreting DTI data. While animal literature provides some ground truth evidence supporting actual and specific corticostriatal projections that are relevant to stuttering neurophysiology and theoretical models, DTI can only provide a probable estimation of neuronal connectivity (Parker 2002; Dauguet 2007). Though these measures are still clearly of biological interest there remains considerable uncertainty.

The stuttering and control groups differed significantly on their Verbal IQ, PPVT, and EVT scores, suggesting that they differed in lexical/semantic processing skills. These differences were largely influenced by some high scorerers in the control group and do not reflect deficits in this skill in CWS (all children in both groups showed scores well within, or exceeding, age norms). Entering Verbal IQ as a covariate in the analyses did not alter our main findings. Nevertheless, we acknowledge that subtle differences in language processing between the two groups may influence the connectivity patterns particularly in the left hemisphere. Future studies will continue to monitor any significant group differences in language scores, which may lead to confirming, expanding, or refuting the present findings.

The initial inclusion criteria for children entering the study required that children do not have a diagnosis of other comorbid neurodevelopmental disorder (this was later modified to include

these children, but still exclude those on medications that affect CNS function). We acknowledge that only including "pure" cases of stuttering do not represent the general population of stuttering children, who have been reported to exhibit higher rates of comorbid developmental issues such as ADHD, anxiety, dyslexia, and speech sound disorders (Iverach et al. 2016; Choo et al. 2020; Unicomb et al. 2020; Boyce et al. 2022). In future studies, it would be important to be cognizant and address previous sampling issues to ensure that a representative group of CWS are included. These efforts will likely require collaborations and formation of consortiums across labs to acquire large sample sizes of children to allow robust statistical analyses of any subgroups that may be present in the stuttering population.

Finally, here we used functionally defined parcels based on fMRI studies with adults. One cannot exclude that the functional segregation of left and right posterior IFCop differs in CWS due to still-developing cognitive and sensorimotor systems.

Conclusions

This study compared white matter connectivity patterns of the bilateral IFC in young CWS relative to children who do not stutter, leveraging functionally segregated parcels within cytoarchitectonically defined area 44 of IFCop. We highlight 2 major findings: First, CWS showed reduced connectivity between the left IFCop (regardless of parcel) and the putamen, corroborating previous empirical and theoretical accounts pointing to deficits in the basal ganglia thalamocortical loop in stuttering. The current results suggest deficits in corticostriatal projections that lead to insufficient cortical input to putaminal neurons, which in turn may negatively impact integration of contextual and kinematic information necessary to secure fluid automatized speech motor execution. Second, here we show for the first time that CWS who are relatively close to stuttering onset, particularly boys, show connectivity patterns indicating both excessive as well as reduced integration of the right posterior IFCop. Specifically, stuttering boys showed increased connectivity of the insular and somatomotor cortices with right IFCop parcels supporting somatomotor and inhibition functions but decreased connectivity with an IFCop parcel associated with dorsal attention. These findings suggest the involvement of not only altered somatomotor but also cognitive (attention, inhibition) processes in stuttering, though whether these differences are associated with compensatory or maladaptive changes remains to be confirmed in future studies. The present findings provide a foundation for further investigations that probe these questions, perhaps best pursued with longitudinal studies of CWS.

Acknowledgments

The authors wish to thank all the children and parents who participated in this research. We wish to also thank Kristin Hicks, Megan Sheppard, and Saralyn Rubsam for their contributions to conducting standardized testing and collecting MRI data, and to Yiling Liu who contributed to preliminary data analyses.

Supplementary material

Supplementary material is available at *Cerebral Cortex* online.

Funding

Conflict of interest statement: The authors declare that they have no known competing financial interests or personal relationships that could have appeared to influence the work reported in this paper.

References

Ackermann H, Riecker A. The contribution(s) of the insula to speech production: a review of the clinical and functional imaging literature. *Brain Struct Funct*. 2010:214:419–433.

Afif A, Minotti L, Kahane P, Hoffmann D. Anatomofunctional organization of the insular cortex: a study using intracerebral electrical stimulation in epileptic patients. *Epilepsia*. 2010:51:2305–2315.

Alm PA. Stuttering and the basal ganglia circuits: a critical review of possible relations. *J Commun Disord*. 2004:37(4):325–369.

Alm PA. The dopamine system and automatization of movement sequences: a review with relevance for speech and stuttering. *Front Hum Neurosci*. 2021:15:661880:1-17.

Amunts K, Schleicher A, Bürgel U, Mohlberg H, Uylings HBM, Zilles K. Broca's region revisited: cytoarchitecture and intersubject variability. *J Comp Neurol*. 1999:412:319–341.

Amunts K, Weiss PH, Mohlberg H, Pieperhoff P, Eickhoff S, Gurd JM, Marshall JC, Shah NJ, Fink GR, Zilles K. Analysis of neural mechanisms underlying verbal fluency in cytoarchitectonically defined stereotaxic space—the roles of Brodmann areas 44 and 45. *NeuroImage*. 2004:22:42–56.

Amunts K, Lenzen M, Friederici AD, Schleicher A, Morosan P, Palomero-Gallagher N, Zilles K. Broca's region: novel organizational principles and multiple receptor mapping. *PLoS Biol*. 2010:8:e1000489.

Andersson JLR, Sotiropoulos SN. An integrated approach to correction for off-resonance effects and subject movement in diffusion MR imaging. *NeuroImage*. 2016:125:1063–1078.

Andersson JLR, Graham MS, Zsoldos E, Sotiropoulos SN. Incorporating outlier detection and replacement into a non-parametric framework for movement and distortion correction of diffusion MR images. *NeuroImage*. 2016:141:556–572.

Aron AR, Poldrack RA. Cortical and subcortical contributions to stop signal response inhibition: role of the subthalamic nucleus. *J Neurosci*. 2006:26:2424–2433.

Baier B, Eulenburg P z, Glassl O, Dieterich M. Lesions to the posterior insular cortex cause dysarthria. *Eur J Neurol*. 2011:18:1429–1431.

Baldo JV, Wilkins DP, Ogar J, Willock S, Dronkers NF. Role of the precentral gyrus of the insula in complex articulation. *Cortex*. 2011:47:800–807.

Bates E, Wilson SM, Saygin AP, Dick F, Sereno MI, Knight RT, Dronkers NF. Voxel-based lesion–symptom mapping. *Nat Neurosci*. 2003:6: 448–450.

Behrens TEJ, Berg HJ, Jbabdi S, Rushworth MFS, Woolrich MW. Probabilistic diffusion tractography with multiple fibre orientations: what can we gain? *NeuroImage*. 2007:34:144–155.

Bernhardt BC, Singer T. The neural basis of empathy. *Annu Rev Neurosci*. 2012:35:1–23.

Bloodstein O, Ratner NB. *A handbook on stuttering*, 552. Clifton Park, NY: Thomson/Delmar Learning; 2008

Bohland JW, Bullock D, Guenther FH. Neural representations and mechanisms for the performance of simple speech sequences. *J Cognitive Neurosci*. 2010:22:1504–1529.

Boyce JO, Jackson VE, Reyk O, Parker R, Vogel AP, Eising E, Horton SE, Gillespie NA, Scheffer IE, Amor DJ, et al. Self-reported impact of

developmental stuttering across the lifespan. *Dev Medicine Child Neurology*. 2022:0:1–10.

Brodmann K. *Vergleichende Lokalisationslehre der Grosshirnrinde in ihren Prinzipien dargestellt auf Grund des Zellenbaues*. Leipzig: Barth; 1909

Brown S, Ingham RJ, Ingham JC, Laird AR, Fox PT. Stuttered and fluent speech production: an ALE meta-analysis of functional neuroimaging studies. *Hum Brain Mapp*. 2005:25:105–117.

Busan P, Ben GD, Russo LR, Bernardini S, Natarelli G, Arcara G, Manganotti P, Battaglini PP. Stuttering as a matter of delay in neural activation: a combined TMS/EEG study. *Clin Neurophysiol*. 2019:130:61–76.

Cai S, Tourville JA, Beal DS, Perkell JS, Guenther FH, Ghosh SS. Diffusion imaging of cerebral white matter in persons who stutter: evidence for network-level anomalies. *Front Hum Neurosci*. 2014:8:54.

Cardinal RN, Parkinson JA, Hall J, Everitt BJ. Emotion and motivation: the role of the amygdala, ventral striatum, and prefrontal cortex. *Neurosci Biobehav Rev*. 2002:26:321–352.

Catani M, Mesulam M. The arcuate fasciculus and the disconnection theme in language and aphasia: history and current state. *Cortex*. 2008:44:953–961.

Catani M, Jones DK, ffytche DH. Perisylvian language networks of the human brain. *Ann Neurol*. 2005:57:8–16.

Catani M, Mesulam MM, Jakobsen E, Malik F, Martersteck A, Wieneke C, Thompson CK, de Schotten MT, Dell'Acqua F, Weintraub S, et al. A novel frontal pathway underlies verbal fluency in primary progressive aphasia. *Brain J Neurology*. 2013:136:2619–2628.

Chambers CD, Bellgrove MA, Stokes MG, Henderson TR, Garavan H, Robertson IH, Morris AP, Mattingley JB. Executive "brake failure" following deactivation of human frontal lobe. *J Cognitive Neurosci*. 2006:18:444–455.

Chambers CD, Bellgrove MA, Gould IC, English T, Garavan H, McNaught E, Kamke M, Mattingley JB. Dissociable mechanisms of cognitive control in prefrontal and premotor cortex. *J Neurophysiol*. 2007:98:3638–3647.

Chang S-E, Guenther FH. Involvement of the cortico-basal ganglia-thalamocortical loop in developmental stuttering. *Front Psychol*. 2020:10:3088.

Chang S-E, Zhu DC. Neural network connectivity differences in children who stutter. *Brain*. 2013:136:3709–3726.

Chang S-E, Kenney MK, Loucks TMJ, Ludlow CL. Brain activation abnormalities during speech and non-speech in stuttering speakers. *NeuroImage*. 2009:46:201–212.

Chang S-E, Horwitz B, Ostuni J, Reynolds R, Ludlow CL. Evidence of left inferior frontal–premotor structural and functional connectivity deficits in adults who stutter. *Cereb Cortex*. 2011:21: 2507–2518.

Chang S-E, Zhu DC, Choo AL, Angstadt M. White matter neuroanatomical differences in young children who stutter. *Brain*. 2015:138:694–711.

Chang S-E, Chow HM, Wieland EA, McAuley JD. Relation between functional connectivity and rhythm discrimination in children who do and do not stutter. *Neuroimage Clin*. 2016:12: 442–450.

Chang S-E, Angstadt M, Chow HM, Etchell AC, Garnett EO, Choo AL, Kessler D, Welsh RC, Sripada C. Anomalous network architecture of the resting brain in children who stutter. *J Fluen Disord*. 2018:55: 46–67.

Chikama M, McFarland NR, Amaral DG, Haber SN. Insular cortical projections to functional regions of the striatum correlate with cortical cytoarchitectonic organization in the primate. *J Neurosci*. 1997:17:9686–9705.

Choo AL, Smith SA, Li H. Associations between stuttering, comorbid conditions and executive function in children: a population-based study. *BMC Psychology*. 2020:8:113.

Chow HM, Chang S. White matter developmental trajectories associated with persistence and recovery of childhood stuttering. *Hum Brain Mapp*. 2017:38:3345–3359.

Civier O, Bullock D, Max L, Guenther FH. Computational modeling of stuttering caused by impairments in a basal ganglia thalamo-cortical circuit involved in syllable selection and initiation. *Brain Lang*. 2013:126:263–278.

Cler GJ, Krishnan S, Papp D, Wiltshire CEE, Chesters J, Watkins &KE. Elevated iron concentration in putamen and cortical speech motor network in developmental stuttering. *Brain*. 2021:144: 2979–2984.

Clos M, Amunts K, Laird AR, Fox PT, Eickhoff SB. Tackling the multifunctional nature of Broca's region meta-analytically: co-activation-based parcellation of area 44. *NeuroImage*. 2013:83: 174–188.

Connally EL, Ward D, Howell P, Watkins KE. Disrupted white matter in language and motor tracts in developmental stuttering. *Brain Lang*. 2014:131:25–35.

Craig AD. How do you feel — now? The anterior insula and human awareness. *Nat Rev Neurosci*. 2009:10:59–70.

Cykowski MD, Fox PT, Ingham RJ, Ingham JC, Robin DA. A study of the reproducibility and etiology of diffusion anisotropy differences in developmental stuttering: a potential role for impaired myelination. *NeuroImage*. 2010:52:1495–1504.

Dauguet J, Peled S, Berezovskii V, Delzescaux T, Warfield SK, Born R, Westin C-F. Comparison of fiber tractsderived from in-vivo DTI tractography with 3D histological neural tract tracerreconstruction on a macaque brain. *Neuroimage*. 2007:37:530–538.

Deacon TW. Cortical connections of the inferior arcuate sulcus cortex in the macaque brain. *Brain Res*. 1992:573:8–26.

Desai J, Huo Y, Wang Z, Bansal R, Williams SCR, Lythgoe D, Zelaya FO, Peterson BS. Reduced perfusion in Broca's area in developmental stuttering. *Hum Brain Mapp*. 2017:38:1865–1874.

Dick AS, Garic D, Graziano P, Tremblay P. The frontal aslant tract (FAT) and its role in speech, language and executive function. *Cortex*. 2018:111:148–163.

Donaher J, Richels C. Traits of attention deficit/hyperactivity disorder in school-age children who stutter. *J Fluen Disord*. 2012:37:242–252.

Dronkers NF. A new brain region for coordinating speech articulation. *Nature*. 1996:384:159–161.

Duffau H, Taillandier L, Gatignol P, Capelle L. The insular lobe and brain plasticity: lessons from tumor surgery. *Clin Neurol Neurosur*. 2006:108:543–548.

Dunn DM, Dunn LM. *Peabody picture vocabulary test: manual*. Minneapolis, MN: Pearson; 2007

Eggers K, Nil LFD, den BRHV B. Inhibitory control in childhood stuttering. *J Fluen Disord*. 2013:38:1–13.

Evans AC, Janke AL, Collins DL, Baillet S. Brain templates and atlases. *NeuroImage*. 2012:62:911–922.

Fedorenko E, Fillmore P, Smith K, Bonilha L, Fridriksson J. The superior precentral gyrus of the insula does not appear to be functionally specialized for articulation. *J Neurophysiol*. 2015:113: 2376–2382.

Ferpozzi V, Fornia L, Montagna M, Siodambro C, Castellano A, Borroni P, Riva M, Rossi M, Pessina F, Bello L, et al. Broca's area as a pre-articulatory phonetic encoder: gating the motor program. *Front Hum Neurosci*. 2018:12:64.

Finkl T, Hahne A, Friederici AD, Gerber J, Mürbe D, Anwander A. Language without speech: segregating distinct circuits in the human brain. *Cereb Cortex*. 2019:30:812–823.

Flinker A, Korzeniewska A, Shestyuk AY, Franaszczuk PJ, Dronkers NF, Knight RT, Crone NE. Redefining the role of Broca's area in speech. *Proc Natl Acad Sci*. 2015:112:2871–2875.

Fox PT, Ingham RJ, Ingham JC, Hirsch TB, Downs JH, Martin C, Jerabek P, Glass T, Lancaster JL. A PET study of the neural systems of stuttering. *Nature*. 1996:382:158–162.

Garnett EO, Chow HM, Nieto-Castañón A, Tourville JA, Guenther FH, Chang S-E. Anomalous morphology in left hemisphere motor and premotor cortex of children who stutter. *Brain*. 2018:141: 2670–2684.

Geschwind N, Galaburda AM. Cerebral lateralization: biological mechanisms, associations, and pathology: II. A hypothesis and a program for research. *Arch Neurol*. 1985:42:521.

Gilmore M, Harcourt S, Strong A, Cabrera C, Golden C. B-28 How well do PPVT-4, EVT-2, and NDRT vocabulary subtest predict WAIS-IV indices and FSIQ. *Arch Clin Neuropsych*. 2018:33: 703–794.

Giraud A-L, Neumann K, Bachoud-Levi A-C, von Gudenberg AW, Euler HA, Lanfermann H, Preibisch C. Severity of dysfluency correlates with basal ganglia activity in persistent developmental stuttering. *Brain Lang*. 2008:104:190–199.

Goldman R. *Goldman-Fristoe test of articulation (GFTA-2)*. Circle Pines, MN: American Guidance Service, Inc.; 2000

Guenther FH. Cortical interactions underlying the production of speech sounds. *J Commun Disord*. 2006:39:350–365.

Guenther FH. *Neural control of speech*; 2016. Cambridge, MA: MIT Press.

Haber SN. Corticostriatal circuitry. *Dialogues Clin Neurosci*. 2016:18: 7–21.

Hannah R, Muralidharan V, Sundby KK, Aron AR. Temporally-precise disruption of prefrontal cortex informed by the timing of beta bursts impairs human action-stopping. *NeuroImage*. 2020:222: 117222–117222.

Hartwigsen G, Neef NE, Camilleri JA, Margulies DS, Eickhoff SB. Functional segregation of the right inferior frontal gyrus: evidence from coactivation-based parcellation. *Cereb Cortex*. 2019:29: 1532–1546.

Hickok G, Poeppel D. The cortical organization of speech processing. *Nat Rev Neurosci*. 2007:8:393–402.

Hickok G, Houde J, Rong F. Sensorimotor integration in speech processing: computational basis and neural organization. *Neuron*. 2011:69:407–422.

Hillis AE, Work M, Barker PB, Jacobs MA, Breese EL, Maurer K. Reexamining the brain regions crucial for orchestrating speech articulation. *Brain*. 2004:127:1479–1487.

Hollingshead AB. *Four-factor index of social status*; 1975. New Haven, CT: Yale University.

Howell P, Jiang J, Peng D, Lu C. Neural control of rising and falling tones in Mandarin speakers who stutter. *Brain Lang*. 2012:123: 211–221.

Hughes ME, Johnston PJ, Fulham WR, Budd TW, Michie PT. Stopsignal task difficulty and the right inferior frontal gyrus. *Behav Brain Res*. 2013:256:205–213.

Ingham RJ, Wang Y, Ingham JC, Bothe AK, Grafton ST. Regional brain activity change predicts responsiveness to treatment for stuttering in adults. *Brain Lang*. 2013:127:510–519.

Isnard J, Guénot M, Sindou M, Mauguière F. Clinical manifestations of insular lobe seizures: a stereo-electroencephalographic study. *Epilepsia*. 2004:45:1079–1090.

Iverach L, Jones M, McLellan LF, Lyneham HJ, Menzies RG, Onslow M, Rapee RM. Prevalence of anxiety disorders among children who stutter. *J Fluen Disord*. 2016:49:13–28.

Jäncke L, Hänggi J, Steinmetz H. Morphological brain differences between adult stutterers and non-stutterers. *BMC Neurol*. 2004:4:23.

Jenson D, Reilly KJ, Harkrider AW, Thornton D, Saltuklaroglu T. Trait related sensorimotor deficits in people who stutter: an EEG investigation of μ rhythm dynamics during spontaneous fluency. *Neuroimage Clin*. 2018:19:690–702.

Jenson D, Bowers AL, Hudock D, Saltuklaroglu T. The application of EEG mu rhythm measures to neurophysiological research in stuttering. *Front Hum Neurosci*. 2020:13:458.

Jossinger S, Kronfeld-Duenias V, Zislis A, Amir O, Ben-Shachar M. Speech rate association with cerebellar white-matter diffusivity in adults with persistent developmental stuttering. *Brain Struct Funct*. 2021:226:801–816.

Kell CA, Neumann K, von Kriegstein K, Posenenske C, von Gudenberg AW, Euler H, Giraud A-L. How the brain repairs stuttering. *Brain*. 2009:132:2747–2760.

Kell CA, Neumann K, Behrens M, Gudenberg AW v, Giraud A-L. Speaking-related changes in cortical functional connectivity associated with assisted and spontaneous recovery from developmental stuttering. *J Fluen Disord*. 2018:55:135–144.

Klugah-Brown B, Wang P, Jiang Y, Becker B, Hu P, Uddin LQ, Biswal B. Structural-functional connectivity mapping of the insular cortex: a combined data-driven and meta-analytic topic mapping. *Cereb Cortex New York N Y*. 2022:1–13.

Koedoot C, Bouwmans C, Franken M-C, Stolk E. Quality of life in adults who stutter. *J Commun Disord*. 2011:44:429–443.

Korponay C, Choi EY, Haber SN. Corticostriatal projections of Macaque area 44. *Cereb Cortex Commun*. 2020:1:1–11.

Korponay C, Stein EA, Ross TJ. Laterality hotspots in the striatum. *Cereb Cortex New York N Y*. 2021:32:2943–2956.

Krasileva KE, Sanders SJ, Bal VH. Peabody picture vocabulary test: proxy for verbal IQ in genetic studies of autism spectrum disorder. *J Autism Dev Disord*. 2017:47:1073–1085.

Kronfeld-Duenias V, Amir O, Ezrati-Vinacour R, Civier O, Ben-Shachar M. The frontal aslant tract underlies speech fluency in persistent developmental stuttering. *Brain Struct Funct*. 2016a:221: 365–381.

Kronfeld-Duenias V, Amir O, Ezrati-Vinacour R, Civier O, Ben-Shachar M. Dorsal and ventral language pathways in persistent developmental stuttering. *Cortex*. 2016b:81:79–92.

Kronfeld-Duenias V, Civier O, Amir O, Ezrati-Vinacour R, Ben-Shachar M. White matter pathways in persistent developmental stuttering: lessons from tractography. *J Fluen Disord*. 2018:55: 68–83.

Kurth F, Zilles K, Fox PT, Laird AR, Eickhoff SB. A link between the systems: functional differentiation and integration within the human insula revealed by meta-analysis. *Brain Struct Funct*. 2010:214:519–534.

Liman J, von Gudenberg AW, Baehr M, Paulus W, Neef NE, Sommer M. Enlarged area of mesencephalic iron deposits in adults who stutter. *Front Hum Neurosci*. 2021:15:639269.

Loh KK, Procyk E, Neveu R, Lamberton F, Hopkins WD, Petrides M, Amiez C. Cognitive control of orofacial motor and vocal responses in the ventrolateral and dorsomedial human frontal cortex. *Proc Natl Acad Sci*. 2020:117:4994–5005.

Long MA, Katlowitz KA, Svirsky MA, Clary RC, Byun TM, Majaj N, Oya H, Howard MA, Greenlee JDW. Functional segregation of cortical regions underlying speech timing and articulation. *Neuron*. 2016:89:1187–1193.

Lu C, Chen C, Ning N, Ding G, Guo T, Peng D, Yang Y, Li K, Lin C. The neural substrates for atypical planning and execution of word production in stuttering. *Exp Neurol*. 2010:221:146–156.

Lu C, Peng D, Chen C, Ning N, Ding G, Li K, Yang Y, Lin C. Altered effective connectivity and anomalous anatomy in the basal ganglia-thalamocortical circuit of stuttering speakers. *Cortex*. 2010:46: 49–67.

Lu C, Long Y, Zheng L, Shi G, Liu L, Ding G, Howell P. Relationship between speech production and perception in people who stutter. *Front Hum Neurosci*. 2016:10:224.

Mandelli ML, Caverzasi E, Binney RJ, Henry ML, Lobach I, Block N, Amirbekian B, Dronkers N, Miller BL, Henry RG, et al. Frontal white matter tracts sustaining speech production in primary progressive aphasia. *J Neurosci*. 2014:34:9754–9767.

Månsson H. Childhood stuttering incidence and development. *J Fluen Disord*. 2000:25:47–57.

Margulies DS, Petrides M. Distinct parietal and temporal connectivity profiles of ventrolateral frontal areas involved in language production. *J Neurosci*. 2013:33:16846–16852.

Max L, Guenther FH, Gracco VL, Ghosh SS, Wallace ME. Unstable or insufficiently activated internal models and feedback-biased motor control as sources of dysfluency: a theoretical model of stuttering. *Contemp Issues Commun Sci Disord*. 2004:31:105–122.

Mayer M. *Frog, where are you?* New York, NY: Penguin Putnam Inc; 1969

Metzger FL, Auer T, Helms G, Paulus W, Frahm J, Sommer M, Neef NE. Shifted dynamic interactions between subcortical nuclei and inferior frontal gyri during response preparation in persistent developmental stuttering. *Brain Struct Funct*. 2018:223:165–182.

Montag C, Bleek B, Reuter M, Müller T, Weber B, Faber J, Markett S. Ventral striatum and stuttering: robust evidence from a case-control study applying DARTEL. *Neuroimage Clin*. 2019:23:101890.

Neef NE, Paulus W, Neef A, von Gudenberg AW, Sommer M. Reduced intracortical inhibition and facilitation in the primary motor tongue representation of adults who stutter. *Clin Neurophysiol*. 2011:122:1802–1811.

Neef NE, Hoang TNL, Neef A, Paulus W, Sommer M. Speech dynamics are coded in the left motor cortex in fluent speakers but not in adults who stutter. *Brain*. 2015:138:712–725.

Neef NE, Bütfering C, Anwander A, Friederici AD, Paulus W, Sommer M. Left posterior-dorsal area 44 couples with parietal areas to promote speech fluency, while right area 44 activity promotes the stopping of motor responses. *NeuroImage*. 2016:142:628–644.

Neef N, Anwander A, Bütfering C, Schmidt-Samoa C, Friederici AD, Paulus W, Sommer M. Structural connectivity of right frontal hyperactive areas scales with stuttering severity. *Brain*. 2018:141:191–204.

Neef NE, Bütfering C, Auer T, Metzger FL, Euler HA, Frahm J, Paulus W, Sommer M. Altered morphology of the nucleus accumbens in persistent developmental stuttering. *J Fluen Disord*. 2018:55:84–93.

Neumann K, Euler HA, von Gudenberg AW, Giraud A-L, Lanfermann H, Gall V, Preibisch C. The nature and treatment of stuttering as revealed by fMRI a within- and between-group comparison. *J Fluen Disord*. 2003:28:381–410.

Neumann K, Euler HA, Kob M, von Gudenberg AW, Giraud A-L, Weissgerber T, Kell CA. Assisted and unassisted recession of functional anomalies associated with dysprosody in adults who stutter. *J Fluen Disord*. 2018:55:120–134.

Nieuwenhuys R. The insular cortex: a review. *Prog Brain Res*. 2012:195:123–163.

Ogar J, Willock S, Baldo J, Wilkins D, Ludy C, Dronkers N. Clinical and anatomical correlates of apraxia of speech. *Brain Lang*. 2006:97:343–350.

Oh A, Duerden EG, Pang EW. The role of the insula in speech and language processing. *Brain Lang*. 2014:135:96–103.

Oldfield RC. The assessment and analysis of handedness: the Edinburgh inventory. *Neuropsychologia*. 1971:9:97–113.

Parker GJM, Stephan KE, Barker GJ, Rowe JB, MacManus DG, Wheeler-Kingshott CAM, Ciccarelli O, Passingham RE, Spinks RL, Lemon RN, et al. Initial Demonstration of inVivo Tracing of Axonal Projections in the Macaque Brain and Comparison with the Human Brain Using Diffusion Tensor Imaging and Fast Marching Tractography. *Neuroimage*. 2002:15:797–809.

Petrides M, Pandya DN. Distinct parietal and temporal pathways to the homologues of Broca's area in the monkey. *PLoS Biol*. 2009:7:e1000170.

Pimentel-Farfan AK, Báez-Cordero AS, Peña-Rangel TM, Rueda-Orozco PE. Cortico-striatal circuits for bilaterally coordinated movements. *Sci Adv*. 2022:8:eabk2241.

Preibisch C, Neumann K, Raab P, Euler HA, von Gudenberg AW, Lanfermann H, Giraud A-L. Evidence for compensation for stuttering by the right frontal operculum. *NeuroImage*. 2003:20:1356–1364.

Reilly S, Onslow M, Packman A, Wake M, Bavin EL, Prior M, Eadie P, Cini E, Bolzonello C, Ukoumunne OC. Predicting stuttering onset by the age of 3 years: a prospective, community cohort study. *Pediatrics*. 2009:123:270–277.

Riley GD. *SSI-4: stuttering severity instrument*. 4th ed; 2009. Austin, TX: Pro-Ed.

Riley J, Riley JG. A revised component model for diagnosing and treating children who stutter. *Contemp Issues Commun Sci Disord*. 2000:27:188–199.

Rueda-Orozco PE, Robbe D. The striatum multiplexes contextual and kinematic information to constrain motor habits execution. *Nat Neurosci*. 2015:18:453–460.

Sahin NT, Pinker S, Cash SS, Schomer D, Halgren E. Sequential processing of lexical, grammatical, and phonological information within Broca's area. *Science*. 2009:326:445–449.

Salmelin R, Schnitzler A, Schmitz F, Freund H-J. Single word reading in developmental stutterers and fluent speakers. *Brain*. 2000:123:1184–1202.

Sarubbo S, Benedictis AD, Merler S, Mandonnet E, Balbi S, Granieri E, Duffau H. Towards a functional atlas of human white matter. *Hum Brain Mapp*. 2015:36:3117–3136.

Schwartze M, Tavano A, Schröger E, Kotz SA. Temporal aspects of prediction in audition: cortical and subcortical neural mechanisms. *Int J Psychophysiol*. 2012:83:200–207.

Sebastian A, Jung P, Neuhoff J, Wibral M, Fox PT, Lieb K, Fries P, Eickhoff SB, Tüscher O, Mobascher A. Dissociable attentional and inhibitory networks of dorsal and ventral areas of the right inferior frontal cortex: a combined task-specific and coordinate-based meta-analytic fMRI study. *Brain Struct Funct*. 2016:221:1635–1651.

Sebastian A, Rössler K, Wibral M, Mobascher A, Lieb K, Jung P, Tüscher O. Neural architecture of selective stopping strategies: distinct brain activity patterns are associated with attentional capture but not with outright stopping. *J Neurosci*. 2017:37:9785–9794.

Selemon LD, Goldman-Rakic PS. Longitudinal topography and inter-digitation of corticostriatal projections in the rhesus monkey. *J Neurosci Off J Soc Neurosci*. 1985:5:776–794.

Singer CM, Hessling A, Kelly EM, Singer L, Jones RM. Clinical characteristics associated with stuttering persistence: a meta-analysis. *J Speech Lang Hear Res*. 2020:63(9):2995–3018.

Sommer M, Koch MA, Paulus W, Weiller C, Büchel C. Disconnection of speech-relevant brain areas in persistent developmental stuttering. *Lancet*. 2002:360:380–383.

Sowman PF, Ryan M, Johnson BW, Savage G, Crain S, Harrison E, Martin E, Burianová H. Grey matter volume differences in the left caudate nucleus of people who stutter. *Brain Lang*. 2017:164:9–15.

Thompson-Lake DGY, Scerri TS, Block S, Turner SJ, Reilly S, Kefalianos E, Bonthrone AF, Helbig I, Bahlo M, Scheffer IE, et al. Atypical development of Broca's area in a large family with inherited stuttering. *Brain J Neurology*. 2022:145:1177–1188.

Tziortzi AC, Haber SN, Searle GE, Tsoumpas C, Long CJ, Shotbolt P, Douaud G, Jbabdi S, Behrens TEJ, Rabiner EA, et al. Connectivity-based functional analysis of dopamine release in the striatum using diffusion-weighted MRI and positron emission tomography. *Cereb Cortex*. 2014:24:1165–1177.

Uddin LQ. Salience processing and insular cortical function and dysfunction. *Nat Rev Neurosci*. 2015:16:55–61.

Uddin LQ, Nomi JS, Hébert-Seropian B, Ghaziri J, Boucher O. Structure and function of the human insula. *J Clin Neurophysiol*. 2017:34:300–306.

Unicomb R, Kefalianos E, Reilly S, Cook F, Morgan A. Prevalence and features of comorbid stuttering and speech sound disorder at age 4 years. *J Commun Disord*. 2020:84:105976:1–12.

Vogt O. Die myeloarchitektonische Felderung des menschlichen Stirnhirns. *J Psychol Neurol*. 1910:4(5):221–232.

Walsh B, Christ S, Weber C. Exploring relationships among risk factors for persistence in early childhood stuttering. *J Speech Lang Hear Res*. 2021:64:2909–2927.

Warrington S, Bryant KL, Khrapitchev AA, Sallet J, Charquero-Ballester M, Douaud G, Jbabdi S, Mars RB, Sotiropoulos SN. XTRACT - standardised protocols for automated tractography in the human and macaque brain. *NeuroImage*. 2020:217:116923.

Watkins KE, Smith SM, Davis S, Howell P. Structural and functional abnormalities of the motor system in developmental stuttering. *Brain*. 2008:131:50–59.

Wechsler D. *Weschler abbreviated scale of intelligence (WASI)*. London: Psychological Corporation; 1999

Wechsler D. *Wechsler preschool and primary scale of intelligence*. San Antonio, TX: The Psychological Corporation; 2002

Wessel JR, Aron AR. On the globality of motor suppression: unexpected events and their influence on behavior and cognition. *Neuron*. 2017:93:259–280.

Wieland EA, McAuley JD, Dilley LC, Chang S-E. Evidence for a rhythm perception deficit in children who stutter. *Brain Lang*. 2015:144:26–34.

Williams KT. *EVT-2: expressive vocabulary test*. Circle Pines, MN: AGS Publishing; 2007

Winkler AM, Ridgway GR, Webster MA, Smith SM, Nichols TE. Permutation inference for the general linear model. *NeuroImage*. 2014:92:381–397.

Woolnough O, Forseth KJ, Rollo PS, Tandon N. Uncovering the functional anatomy of the human insula during speech. *elife*. 2019:8:e53086.

Wu JC, Maguire G, Riley G, Lee A, Keator D, Tang C, Fallon J, Najafi A. Increased dopamine activity associated with stuttering. *Neuroreport*. 1997:8:767–770.

Wymbs NF, Bassett DS, Mucha PJ, Porter MA, Grafton ST. Differential recruitment of the sensorimotor putamen and frontoparietal cortex during motor chunking in humans. *Neuron*. 2012:74:936–946.

Yairi E, Ambrose N. Epidemiology of stuttering: 21st century advances. *J Fluen Disord*. 2013:38:66–87.

Yang Y, Jia F, Siok WT, Tan LH. Altered functional connectivity in persistent developmental stuttering. *Sci Rep-UK*. 2016:6:19128.

Yaruss JS, Quesal RW. Overall assessment of the speaker's experience of stuttering (OASES): documenting multiple outcomes in stuttering treatment. *J Fluen Disord*. 2006:31:90–115.

Yaruss JS, Quesal RW. *OASES: overall assessment of the speaker's experience of stuttering*. Bloomington: Pearson Assessments; 2014

Yeo BTT, Krienen FM, Sepulcre J, Sabuncu MR, Lashkari D, Hollinshead M, Roffman JL, Smoller JW, Zöllei L, Polimeni JR, et al. The organization of the human cerebral cortex estimated by intrinsic functional connectivity. *J Neurophysiol*. 2011:106:1125–1165.

Zilles K, Amunts K. Cytoarchitectonic and receptorarchitectonic organization in Broca's region and surrounding cortex. *Curr Opin Behav Sci*. 2018:21:93–105.

Zilles K, Bacha-Trams M, Palomero-Gallagher N, Amunts K, Friederici AD. Common molecular basis of the sentence comprehension network revealed by neurotransmitter receptor fingerprints. *Cortex*. 2015:63:79–89.